



HAL
open science

Impact of oysters as top predators on microbial food web dynamics: a modelling approach with parameter optimisation. Running page head: Modelling oyster impact on MFW

R Caillibotte, Y Leredde, F Vidussi, C Ulses, Patrick Marsaleix, C Estournel, Behzad Mostajir

► **To cite this version:**

R Caillibotte, Y Leredde, F Vidussi, C Ulses, Patrick Marsaleix, et al.. Impact of oysters as top predators on microbial food web dynamics: a modelling approach with parameter optimisation. Running page head: Modelling oyster impact on MFW. Marine Ecology Progress Series, 2020, 10.3354/meps13319 . hal-03053199

HAL Id: hal-03053199

<https://hal.science/hal-03053199>

Submitted on 10 Dec 2020

HAL is a multi-disciplinary open access archive for the deposit and dissemination of scientific research documents, whether they are published or not. The documents may come from teaching and research institutions in France or abroad, or from public or private research centers.

L'archive ouverte pluridisciplinaire **HAL**, est destinée au dépôt et à la diffusion de documents scientifiques de niveau recherche, publiés ou non, émanant des établissements d'enseignement et de recherche français ou étrangers, des laboratoires publics ou privés.

1 **Impact of oysters as top predators on microbial food web**
2 **dynamics: a modelling approach with parameter**
3 **optimisation.**

4 **Running page head:** Modelling oyster impact on MFW

5 **R. Caillibotte^{1,*}, Y. Leredde¹, F. Vidussi², C. Ulses³, P. Marsaleix³, C. Estournel³, B.**
6 **Mostajir².**

7 1. Laboratoire Géosciences Montpellier (GM), UMR 5243, CNRS/Université de
8 Montpellier/Université des Antilles. 34090 Montpellier, France.

9 2. Center of Marine Biodiversity, Exploitation and Conservation (MARBEC), UMR 9190,
10 CNRS/ Université de Montpellier/IRD/IFREMER. 34095 Montpellier, France.

11 3. Laboratoire d'Aérodologie (LA), UMR 5560, Université de Toulouse/CNRS/Université Paul
12 Sabatier. 31400 Toulouse, France.

13 **Abstract**

14 Aquaculture is becoming a relevant and productive source of seafood, and production is expected
15 to double in the near future. However, bivalve activities can significantly impact coastal
16 ecosystem functioning. To study the direct and indirect impacts of oysters on the microbial food
17 web, a 0D biogeochemical modelling approach was adopted. The model was adjusted by
18 parameter optimisation, assimilating data from several mesocosm observations of the
19 concentrations of nitrate, phosphate, silicate, dissolved organic carbon and chlorophyll, as well as

* Corresponding author: remi.caillibotte@gm.univ-montp2.fr

1 bacterial biomass. The optimisation method provided a set of optimal parameters to fit the
2 experimental observations of ‘Control’ (i.e., natural water without oysters) and ‘Oyster’ (i.e.,
3 natural water with oysters) mesocosms. The modelling results showed good accordance with the
4 experimental observations, suggesting that the oysters directly reduced the phytoplankton
5 community biomass, thus constraining the ecosystem to a more heterotrophic state. Oysters also
6 reduced the competition between bacteria and phytoplankton for nutrient uptake, favouring a
7 higher bacterial biomass than in the ‘Control’ experiment. Additionally, the presence of oysters
8 strongly increased large micro-zooplankton biomass (50-200 μm , mainly ciliates and large
9 flagellates). This was a consequence of bacterivory by small zooplankton (5-50 μm , mostly
10 flagellates and small ciliates), providing a trophic link between bacteria and larger zooplankton.
11 In conclusion, the parameter optimisation showed a good capacity to manage experimental data
12 in order to build a more realistic model. Such models, in connection with future developments in
13 aquaculture and global change scenarios, could be a promising tool for exploited ecosystem
14 management and testing different environmental scenarios.

15 **Key words:** Oysters, microbial food web, biogeochemical modelling, parameter optimisation,
16 bacteria, phytoplankton, zooplankton, mesocosm.

17 **1 Introduction**

18 Bivalve activities exert a non-neutral influence on coastal ecosystems (e.g., Dupuy et al. 1999,
19 2000, Chapelle et al. 2000, Mostajir et al. 2015), and an increase in the number of shellfish farms
20 in specific areas will certainly impact their nearby ecosystems. The roles of bivalves can be
21 summarised by three main functions (Richard et al. 2019): filtration (Dupuy et al. 2000, Trottet et
22 al. 2008), excretion (Mazouni 2004, Richard et al. 2007, Jansen et al. 2011), and biodeposition

1 (Callier et al. 2006, 2009, Robert et al. 2013). Filtration by oysters selectively removes suspended
2 living or non-living particles from the water column (Gosling 2015, Bayne 2017). Several studies
3 considered the type and size of particles trapped by oysters, ranging from 3 to 5 μm (Barillé et al.
4 1993, Dupuy et al. 1999, 2000) to 500 μm (Barillé et al. 1993, Dupuy et al. 2000, Gosling 2015
5 and references therein), including nano- (3-20 μm) and microplankton (20-200 μm), comprising
6 phyto-, protozo- and metazooplankton. Oyster biodeposition, resulting from faeces and
7 pseudofaeces production (Haven & Morales-Alamo 1966), can also influence the ecosystem as it
8 affects the composition of total particulate matter and nutrient recycling. Souchu et al. (2001),
9 comparing suspended particulate matter and dissolved nutrient distributions between oyster farms
10 and nearby areas not used for cultivation in a Mediterranean lagoon (Thau, France), showed that
11 nitrogen in the biodeposits, which accumulated at the water-sediment interface, was recycled by
12 mineralisation to ammonium, stimulating phytoplankton biomass as a result.

13 In exploited areas, bivalves can modify microbial plankton community structure (e.g., Froján et
14 al. 2014, Mostajir et al. 2015). For example, a mesocosm study was conducted in the
15 northwestern Mediterranean lagoon of Thau (France) to assess the structural and functional
16 impacts of oysters on the microbial food web (MFW) (Mostajir et al. 2015). In this confined
17 environment, the authors analysed the autotroph:heterotroph C biomass ratio (A:H) structural
18 index, indicating that the MFW became more heterotrophic in the presence of oysters as top
19 predators.

20 Several modelling studies have simulated the evolution of oysters or their influence on
21 biogeochemical cycles and other MFW components. Two main categories can be distinguished
22 with diverse approaches and goals. The first category of models is focused on oyster evolution
23 and behaviours in a specified environment, comprising models using the dynamic energy budget

1 (DEB) theory (Kooijman 1986, 2000, 2009) and other population growth models (e.g., Gangnery
2 et al. 2001, 2003, 2004). The second category includes models commonly used to investigate
3 bivalve-environment interactions. This category concerns biogeochemical models integrating
4 oysters, where biogeochemical models describe MFW processes generally forced by the physical
5 environment (e.g., temperature and light). Several studies included the nitrogen and/or
6 phosphorus cycles (Chapelle et al. 2000, Zaldívar et al. 2003). In parallel with these
7 developments and because of the strong coupling between physics and biology, biogeochemical
8 models are regularly coupled with 3D oceanic circulation models (e.g., Auger et al. 2014, Plus et
9 al. 2015, Ulses et al. 2016). Other developments have been made in coupling ecological models
10 of bivalve algorithms with hydrodynamic models to simulate food availability and thus the
11 carrying capacities of bivalve populations (Duarte et al. 2003, Marinov et al. 2007) or the impact
12 of bivalves on the spatial distribution of phytoplankton (Spillman et al. 2008, Cugier et al. 2010,
13 Ibarra et al. 2014).

14 The present study focused on the interaction between oysters and MFW components and fluxes,
15 using a 0D modelling approach. This work was part of the development of a 3D coupled
16 hydrodynamic-biogeochemical model of an exploited coastal northwestern Mediterranean lagoon
17 (Thau, France). The Thau lagoon is a shallow marine lagoon connected to the sea by three narrow
18 channels. It has been highly exploited for bivalve culture and, in particular, the culture of the non-
19 native oyster *Crassostrea gigas*, which has been cultivated in the lagoon since 1972 (Hamon et
20 al. 2003). The originality of this work lies in the insertion of a new oyster compartment into the
21 highly comprehensive Eco3m-S biogeochemical model, presented in detail in Auger et al. (2011).
22 An optimisation method assimilating mesocosm observations described in Mostajir et al. (2015)
23 was performed to determine the best control parameters for the model. The Eco3m-S

1 biogeochemical model was used to simulate complex ecosystem dynamics composed of several
2 decoupled cycles of biogenic elements (carbon, nitrogen, phosphorus, and silica). The new oyster
3 compartment was implemented to investigate the impact of the insertion of oysters as top
4 predators of the MFW. The mesocosm study of Mostajir et al. (2015) showed very good
5 experimental results regarding MFW structure and functioning resulting from the introduction of
6 oysters, but these results could not be extrapolated. The advantage of the new model is that it
7 provides high-frequency results and deeper insight into interactions and fluxes within the MFW.
8 In further studies, the model could also be used to elucidate the potential response of the
9 ecological system to new environmental conditions and forcings. Future studies involving this
10 new model will use 3D coupled hydrodynamic-biogeochemical modelling of the same study area.
11 Specific questions to be addressed by the current study were (1) What are the essential
12 biogeochemical processes modified within the MFW by the insertion of oysters? (2) What are the
13 direct and indirect impacts of the insertion of oysters on the different components of the MFW?

14 **2 Materials and methods**

15 **2.1 Experimental data**

16 A mesocosm study was conducted at the Mediterranean Centre for Marine Ecosystem
17 Experimental Research (MEDIMEER) (Mostajir et al. 2015) based at the marine station of Sète
18 (southern France). The purpose was to determine the MFW structural and functional responses to
19 oysters as top predators. Four mesocosms filled simultaneously with screened (<1000 µm) natural
20 Thau lagoon surface water were studied over 10 days in October 2005 near the MEDIMEER
21 pontoon. Two of the mesocosms contained only natural water ('Control'), and two contained 10
22 *Crassostrea gigas* each ('Oyster'). These mesocosms mimicked a water column without

1 including a sedimentary compartment. The water column was kept homogeneous by using a
2 pump to assure water column mixing.

3 The present modelling study does not reproduce all observations described in Mostajir et al.
4 (2015) because only a few of them were relevant for the model. Temperature and
5 photosynthetically active radiation (PAR: 400-700 nm) were used as external forcings. Six
6 experimental observations, detailed below, were used to initialise the numerical model on day 0
7 (beginning of the mesocosm experiment) and for parameter optimisation thereafter.

8 Temperature (fig. 1) was measured every 10 minutes throughout the mesocosm experiment. PAR
9 (fig. 1) was recorded every 10 minutes, between 14:00 on day 0 and 23:50 on day 7. Then, on day
10 8, measurements were stopped due to sensor failure. However, to complete our model's forcings,
11 the observed values obtained on day 7 were replicated on days 8 and 9. Nutrient concentration
12 data (nitrate (μM): fig. 2-A and 3-A, phosphate (μM): fig. 2-B and 3-B, silicate (μM): fig. 2-C
13 and 3-C) as well as dissolved organic carbon concentration (DOC) data (μM : fig. 2-D and 3-D)
14 were determined with samples taken once a day at 10:00 from day 1 until day 9. Chlorophyll *a*
15 (Chl *a*) concentration in mg m^{-3} (fig. 2-E and 3-E) was measured using high-performance liquid
16 chromatography (HPLC). Bacterial abundances measured by flow cytometry were converted to C
17 biomass (in $\text{mmol of carbon m}^{-3}$, fig. 2-F and 3-F) using a factor of $20 \text{ fg C bacterium}^{-1}$ (Sime-
18 Ngando et al. 1995, Vidussi et al. 2011). More details on this study can be found in Mostajir et al.
19 (2015).

20 **2.2 Model description and initial simulation**

21 The Eco3m-S biogeochemical model used in this study is presented in detail in Auger et al.
22 (2011). It was built to simulate the temporal evolution of a complex ecosystem composed of

1 several decoupled cycles of biogenic elements (carbon, nitrogen, phosphorus, and silica), with a
2 mechanistic approach for biogeochemical processes. A schematic view of the model is presented
3 in fig. 4. The Eco3m-S model includes 36 variables, including photoautotroph and heterotroph
4 biomasses, non-living particulate organic matter (POM) concentration, dissolved organic matter
5 concentration, and nutrient and oxygen concentrations (detailed in Table 1). It also includes 166
6 fundamental control parameters, in the case without oysters, defining the modelled
7 biogeochemical processes. As an example, the model requires 10 parameters to define the grazing
8 function of the first zooplankton size class (5-50 μm).

9 The model is composed of several plankton groups characterised by their functional type,
10 resulting from an analysis of experimental and modelling information on the biogeochemical
11 functioning of the NW Mediterranean Sea. Autotrophs included three size classes of
12 phytoplankton, namely, 0.7-2 μm (Phy₁), 2-20 μm (Phy₂) and 20-200 μm (Phy₃, largely
13 dominated by silicifiers such as diatoms), while heterotrophs included four size classes, namely,
14 0.3-1 μm (mainly bacteria), 5-50 μm (Zoo₁, mostly bacterivorous flagellates and small ciliates),
15 50-200 μm (Zoo₂, mainly ciliates and large flagellates), and >200 μm (Zoo₃, metazooplankton
16 dominated by copepods). To ease the comparison with the total Chl *a* concentration
17 measurements, only one group of phytoplankton (Phy) was considered in our study, representing
18 the entire phytoplankton community. The initial parameters of this group were similar to the
19 parameter values of the third phytoplankton size class (Phy₃) because diatoms dominated the
20 phytoplankton community during the mesocosm experiment. Optimal parameters obtained by our
21 method thus correspond to the total phytoplankton community. However, the three types of
22 zooplankton were maintained in the model as they predate on different groups of living

1 organisms (bacteria, phytoplankton and even smaller zooplankton) or non-living POM (see fig.
2 5).

3 Four types of dissolved inorganic nutrients were considered: nitrate (NO_3^-), ammonium (NH_4^+),
4 phosphate (PO_4^{3-}) and silicate (SiO_4^{2-}). The distinct roles of nitrate and ammonium, which are
5 involved in new and regenerated production, were taken into account. Dissolved organic matter
6 (DOM), in the forms of carbon (C), nitrogen (N) and phosphorus (P), was also considered as it
7 was consumed by heterotrophic bacteria. Non-living POM, in the forms of C, N, P, and Si, was
8 divided into two size classes: $<50 \mu\text{m}$ (light) and $>50 \mu\text{m}$ (heavy). Light non-living POM was
9 also in the form of chlorophyll, resulting from phytoplankton death and zooplankton egestion.
10 The model could also include particulate inorganic matter, which contributes to turbidity and
11 light absorption.

12 Experimental observations of nutrients, DOC, bacteria and Chl *a* on day 0 fixed some of the
13 initial conditions required for running the model. Without any information on non-living matter,
14 initial non-living POM concentrations were set to zero at the beginning of the experiment. Since
15 the experimental study did not provide zooplankton biomasses, the initial conditions for Zoo₁,
16 Zoo₂ and Zoo₃ were fixed after calibration. The oxygen concentration was set to be sufficient
17 (200 mmol m^{-3}) to avoid limiting biogeochemical processes because the water column was
18 considered well mixed. Temperature and PAR measured during the mesocosm experiment were
19 used in the model to force biogeochemical processes.

20 Once initial conditions were established and forcings were defined, an initial simulation was
21 performed to simulate the 10 days of the experiment, using parameters suitable for the NW
22 Mediterranean Sea, where the model is usually implemented (Auger et al. 2011). The model can
23 provide daily variations in the 36 variables at a high frequency, typically every 10 minutes, for

1 applied simulation. In fact, this interval of time corresponds to the time step chosen to resolve the
2 differential equations of the model. Biogeochemical fluxes such as primary production, grazing
3 and respiration were extracted as outputs of the model.

4 The results obtained for this initial simulation were then compared with the available data
5 (nitrate: fig. 2-A, phosphate: fig. 2-B, silicate: fig. 2-C, DOC: fig. 2-D, Chl *a*: fig. 2-E, bacteria:
6 fig. 2-F). The model results provided the same orders of magnitude as the experimental data,
7 even though the two sets of magnitudes did not exhibit similar patterns. For instance, the N, P
8 and Si nutrient concentrations were excessively high. However, the N concentrations were
9 similar to the experimental data at the end of the experiment. It should also be noted that bacterial
10 C biomass was reduced to zero after day 4 of the experiment. Because bacteria were involved in
11 the decomposition process and assimilation of DOM, the very low simulated bacterial biomass
12 led to discrepancies between model results and experimental data in terms of nutrients and DOM.
13 The model also provided additional information such as ammonium concentration (fig. 6-A) and
14 zooplankton biomasses (fig. 6-B) for which no corresponding experimental data were measured.

15 **2.3 Optimisation method**

16 To reduce the discrepancies between experimental observations and biogeochemical model
17 results, an optimisation method suggested by Prunet et al. (1996) was adopted. The mesocosm
18 experiment provided a total of 54 experimental observations by the measurement of six variables,
19 once a day, for 9 days (see 2.1; day 0 was used as the initial condition). The Eco3m-S model
20 included 166 parameters controlling biogeochemical processes. The aim of this mathematical
21 method was to modify, namely, optimise, the control parameter values in order to minimise a cost
22 function representing the gap between observations and model results.

1 The ecosystem model was considered an application $M: \mathbb{R}^m \rightarrow \mathbb{R}^n$, where n is the number of
2 experimental observations (here, $n = 54$) and m is the number of parameters ($m = 166$ in the
3 model without oysters). With the application M being non-linear, the component $(p_i)_{1 \leq i \leq m}$ of the
4 control parameter vector P was optimised iteratively to reduce the gap between the observations
5 denoted $(d_j)_{1 \leq j \leq n}$ and the corresponding simulation results denoted $(c_j)_{1 \leq j \leq n}$. The error
6 associated with observation d_j was denoted r_j . This optimisation procedure finally consisted of
7 minimising a quadratic cost criterion (equation 1):

$$F(P) = \sum_{j=1}^n \left(\frac{d_j - c_j}{r_j} \right)^2 \quad (1)$$

8 The value of the cost function was used to determine if the model results became more similar to
9 the experimental observations with the iterative optimisation method. In the present study, for the
10 first iteration, the control parameter values were extracted from the literature (see Auger et al.
11 2011) and corresponded to the initial simulation. P_0 was then defined as the first guess of the
12 iterative method. $P_k \in \mathbb{R}^m$ was defined as the control parameter vector for iteration number k .
13 The vector of the difference between observed and simulated results $(d_j - c_j)$, denoted $R_k \in \mathbb{R}^n$,
14 was introduced. To find the optimal parameters, the aim was to determine $\Delta P = P_{k+1} - P_k$,
15 which solved equation 2:

$$M'(P_k) \times \Delta P = R_k \quad (2)$$

1 $M'(P_k)$ is the tangent application of M evaluated at point P_k . $M'(P_k) = \left(\frac{\partial c_j}{\partial p_i} \right)_{\substack{1 \leq j \leq n \\ 1 \leq i \leq m}}$, with a
 2 dimension of $n \times m$, is also called the Jacobian matrix of the system. This yields the system of
 3 unknowns Δp_i , with $1 \leq i \leq m$:

$$\sum_{i=1}^m \frac{\partial c_j}{\partial p_i} \times \Delta p_i = d_j - c_j, \text{ for } 1 \leq j \leq n \quad (3)$$

4 Each component $\left(\frac{\partial c_j}{\partial p_i} \right)$ was approximated by $\left(\frac{\delta c_j}{\delta p_i} \right)$ after small explicit perturbations of each
 5 parameter δp_i and compilation of deviations of the model results δc_j . This step required running
 6 the model $(m + 1)$ times at every iteration: a first simulation run without perturbation and then
 7 m simulation runs with only parameter m perturbed. For this reason, the optimisation method
 8 could have a high computational cost. However, in the present work, the duration of a simulation
 9 run was very short and was not limiting in the process.

10 The system must be dimensionless for both parameters and observations. To render the system
 11 dimensionless regarding parameters, a parameter weight diagonal matrix S , containing the a
 12 priori variances of the control parameters, was inserted (equation 4).

$$S_{i,i} = \sigma_i^2, \text{ for } 1 \leq i \leq m \quad (4)$$

13 In the present study, S was practically chosen to reduce $S^{-\frac{1}{2}} \times P_0$ to the vector identity. A weight
 14 diagonal matrix W containing the a priori weight of each observation was also introduced to
 15 render the system dimensionless regarding observations (equation 5).

$$W_{j,j} = \frac{1}{r_j^2}, \text{ for } 1 \leq j \leq n \quad (5)$$

1 W was assumed to be diagonal here, which meant that the observations were uncorrelated. The
 2 advantage of using these two matrices is the ability to choose a more or less important weight for
 3 a specific parameter or observation. Then, equation 6 was obtained from equation 2, introducing
 4 the new weight matrices:

$$W^{-\frac{1}{2}} \times M'(P_k) \times S^{\frac{1}{2}} \times S^{-\frac{1}{2}} \times \Delta P = W^{-\frac{1}{2}} \times R_k \quad (6)$$

5 Equation 6 was an under-determined system $A \times Q = T$, with a number of equations ($n = 54$)
 6 strictly smaller than the number of unknowns ($m = 166$). The matrix $A = W^{-\frac{1}{2}} \times M'(P_k) \times S^{\frac{1}{2}}$
 7 was thus singular, and various combinations of parameters resulted in the same simulation.
 8 Matrix A can be decomposed by singular value decomposition (SVD) as follows:

$$A = U \times L \times V^t \quad (7)$$

9 L is a diagonal matrix of eigenvalues, U is a base of eigenvectors in the space of data, and V is a
 10 base of eigenvectors of parameters. As A was singular, some of the singular values were zero and
 11 defined the null space of the system and thus the rank. In practice, due to numerical computation,
 12 those values were not strictly zero, and the rank was difficult to define. It was typically between 5
 13 and 20. The collinearities between parameters led to a rank deficiency problem, and the pseudo-
 14 inverse was influenced by small eigenvalues. The system was then truncated at rank r using the
 15 sphericity test of Gonzalez Vicente (1986). Without this truncation, the new estimated parameters

1 could be far from their starting point, which was not desirable in terms of keeping the model
2 realistic. The solution was finally calculated using equation 8.

$$\Delta P = S^{\frac{1}{2}} \times V_r \times L_r \times U_r \times W^{-\frac{1}{2}} \times R_k \quad (8)$$

3 V_r , L_r , and U_r were the truncated matrices associated with V , L and U , respectively. The diagonal
4 elements of matrix $(V_r \times V_r^t)$ were estimators of the determination of each control parameter and
5 were called parameter resolutions. The matrix $(U_r \times U_r^t)$ gave similar information for the data,
6 and its diagonal elements were called data resolutions. They showed the contribution of each
7 observation as useful information to the system (e.g., Wunsch 1978).

8 The optimisation procedure involved all 166 parameters. However, in practice, most of them had
9 a weak influence on the results. For example, as noted above (section 2.2), the oxygen
10 concentration was sufficient to avoid limiting biogeochemical processes. Then, the modification
11 of parameters linked with oxygen processes did not affect our results, and the resolutions of these
12 parameters were always null.

13 **2.4 System of equations for oysters**

14 To insert the new compartment for oysters into the ecosystem model, a method inspired by
15 Chapelle et al. (2000) was applied, assuming two main functions. The first function was the
16 filtration of all living (zooplankton, phytoplankton, and bacteria) and non-living (non-living
17 POM) particles. The second function of the new compartment was biodeposition (e.g.,
18 pseudofaeces). These two processes defined the temporal evolution of oyster biomass
19 ($[Oyster]_C$), expressed as carbon concentration (mmol C m^{-3}).

$$\frac{d[Oyster]_c}{dt} = \sum filt_x - biodO \quad (9)$$

1 $filt_x$ is the filtration by oysters of the living and non-living particulate matter X present in the
 2 water column (Bac, Zoo1, Zoo2, Zoo3, Phy, and light and heavy non-living POM). Bacteria were
 3 also considered in the filtration process as they can be attached to larger non-living particulate
 4 matter (Frikha et al. 1987, found in De Crignis 2007), but the efficiency of this filtration was
 5 assumed to be very low (see Table 2). $biodO$ corresponded to the biodeposition of non-living
 6 POM (light and heavy). The first modelling results showed no impact of oyster excretion on the
 7 water column for this specific experimental period. Therefore, this process was not modelled in
 8 this study to reduce the number of control parameters needed and simplify the optimisation
 9 method. The variables and fluxes presented here were first calculated in units of carbon, as were
 10 the processes in other compartments. To include a filtration efficiency $effO_x$ for each filtrated
 11 particle X , the filtration term was expressed as in equation 10.

$$filt_x = \alpha_{filt} \times effO_x \times [X]_c \quad (10)$$

12 The coefficient α_{filt} depended on temperature, oyster biomass and the maximum filtration rate of
 13 oysters $filt_0$.

$$\alpha_{filt} = filt_0 \times f(T) \times [Oyster]_c \quad (11)$$

14 In addition to other temperature-dependent processes, $f(T)$ represented the temperature
 15 limitation of the biological process. It was expressed with the commonly used Q_{10} model (e.g.,
 16 Sherman et al. 2016).

$$f(T) = Q_{10}^{(T_{ref}-T)/10} \quad (12)$$

1 Biodeposition was calculated as a constant percentage of predation (Mazouni 1995, Chapelle et
2 al. 2000).

$$biodO = bd_{\%} \times \sum filt_x \quad (13)$$

3 To impact other compartments of the biogeochemical model, the filtration term was included as a
4 sink term for each filtrated particle, and the biodeposition term was included as a source term for
5 light and heavy non-living POM. A total of 14 new parameters (see Table 2) were introduced to
6 the existing Eco3m-S model in order to control the two main functions of oysters.

7 **3 Results**

8 The results of this study will be presented in two parts. In the first part, the results of the
9 ‘Control’ optimisation, corresponding to the results of the optimisation procedure applied for the
10 initial Eco3m-S model, before the addition of the new oyster compartment, will be presented. The
11 second part will present the results of the ‘Oyster’ optimisation, corresponding to the new
12 biogeochemical model including oysters. Each part will be discussed in three steps: a description
13 of simulation results, an analysis of adjusted parameters, and an analysis of data resolutions.

14 **3.1 ‘Control’ optimisation**

15 The optimisation method was first performed on the original biogeochemical model, without the
16 oyster compartment, using the experimental observations available for the ‘Control’ mesocosms
17 (i.e., including the entire MFW but without oysters). The initial simulation presented in section

1 2.2 was used as the first guess. Similar weights for the observations were imposed (managed by
2 matrix W , see section 2.3). The optimisation sequence, aiming at minimising the cost function
3 and optimising the parameters of the model, was iterated 47 times (i.e., 47×167 simulation runs)
4 until the parameters reached a fixed value and plateaued. The value of the cost function ranged
5 from 1.00 initially to 0.08 at the end. The ‘Control’ optimisation was thus more similar to the
6 experimental observations than the initial simulation was.

7 **3.1.1 Simulation results**

8 Nutrient concentrations for the ‘Control’ optimisation were more similar to the experimental
9 observations than were the initial simulation results. For nitrate concentration (fig. 2-A), the gap
10 between the ‘Control’ optimisation results and observations was $0.03 \mu\text{M}$ on average, whereas
11 the gap was $0.1 \mu\text{M}$ for the initial simulation. The amplitude of daily variations was also reduced
12 by the optimisation procedure. Between days 3 and 4, the concentration ranged from 0.05 to 0.10
13 μM , whereas it was 0.33 to $0.76 \mu\text{M}$ in the initial simulation.

14 Concerning the phosphate concentration (fig. 2-B), from the beginning until day 3, the decrease
15 in phosphate during the daytime was greater in the ‘Control’ simulation than in the initial
16 simulation. However, the increase in phosphate concentration during nights was lower for the
17 optimised simulation. The mean concentration over the entire period was $0.18 \mu\text{M}$ for the
18 optimised simulation, compared to $0.16 \mu\text{M}$ for the experimental observations.

19 The silicate concentration (fig. 2-C) for the ‘Control’ optimisation was lower than that for the
20 initial simulation. The values obtained remained generally larger than the observations, but the
21 trend was well represented. The optimised average concentration throughout the study period was
22 $4.04 \mu\text{M}$, compared to $3.65 \mu\text{M}$ in the initial simulation.

1 The ammonium concentration (fig. 6-A) increased gradually from day 0 (0.3 μM) until day 5 (3.2
2 μM) in the ‘Control’ optimisation. Thereafter, it was stable around a value of 2.6 μM , in contrast
3 to the initial simulation, in which the concentration decreased towards a much lower value (i.e.,
4 0.3 μM at the end of the initial simulation).

5 The DOC concentration (fig. 2-D) in the optimised simulation decreased less than that in the
6 initial simulation and was nearly constant throughout the experimental period. It ranged from 202
7 to 235 μM . The maximum experimental values of DOC observed during days 3 and 4 were not
8 captured by the optimised simulation.

9 Regarding the Chl *a* concentration (fig. 2-E) for the optimised simulation, the results were more
10 similar to the observations than were those obtained with the initial simulation. The simulated
11 results followed the behaviour of measurements taken during the mesocosm experiment. The
12 decrease in Chl *a* concentration on day 3 was corrected by the optimisation procedure to fit the
13 experimental points. From day 5 until the end, the amplitude of the daily variations was almost
14 constant for the ‘Control’ optimisation, with an increase during daytime equal to the decrease
15 during nighttime (approximately 0.6 mg m^{-3}). Hence, the simulation did not reproduce the
16 experimental observations on day 7 but was clearly consistent with the last few days.

17 The most significant improvement was in the bacterial C biomass concentration (fig. 2-F), which
18 showed a good fit with experimental observations for the ‘Control’ optimisation. In contrast to
19 the initial simulation, the values obtained were not reduced to zero after day 4. Note that the
20 bacterial growth during the first few days was higher in the optimised simulation than in the
21 initial simulation. The concentration reached a maximum of 15.73 mmol C m^{-3} on day 2 and a
22 minimum of 4.76 mmol C m^{-3} between days 4 and 5, compared to 15.52 and 4.61 mmol C m^{-3} for
23 the observations, respectively.

1 Zoo₁ and Zoo₂ C biomass concentrations (fig. 6-B) in the ‘Control’ optimisation followed a
2 similar increase for the first two days of the experiment, contrary to those in the initial
3 simulation. Then, the Zoo₂ C biomass concentration exceeded the Zoo₁ concentration, which
4 depicted a link of predation. Between days 2 and 3, the two concentrations reached a maximum
5 (5.26 mmol C m⁻³ for Zoo₁ and 7.97 mmol C m⁻³ for Zoo₂). From day 3 until the end of the
6 experiment, Zoo₁ and Zoo₂ showed similar patterns, and the gap between the two concentrations
7 remained almost constant. At the end, the Zoo₁ and Zoo₂ concentrations were 2.72 and 5.32
8 mmol C m⁻³, respectively. The C biomass concentration of Zoo₃ was almost the same in the
9 ‘Control’ optimisation and the initial simulation.

10 **3.1.2 Analysis of adjusted parameters**

11 The method used in this study estimated the resolution of each parameter, i.e., the importance of
12 each parameter for making the simulated results more similar to the observations. Parameter
13 resolution was used to sort parameters and identify the key parameters for the optimisation
14 procedure (see Table 3). A small change in these parameters can affect the whole biogeochemical
15 simulation. Therefore, the modification of these key parameters by the optimisation procedure
16 was investigated. Table 3 presents a list of key parameters presenting both a high resolution rate
17 and a significant change.

18 Seven parameters among the identified key parameters (Table 3) controlled the zooplankton
19 processes. The *preference factor of micro-zooplankton for nano-zooplankton* and the *maximum*
20 *grazing rate of micro-zooplankton* both increased in the process, with changes of +64% and
21 +86%, respectively. This led to higher predation of Zoo₁ by Zoo₂ in the ‘Control’ simulation
22 compared to that in the initial simulation. This might explain the shifting in time of the maximum

1 Zoo₂ C biomass concentration (fig. 6-B), happening on day 7 in the initial simulation and on day
2 3 in the ‘Control’ simulation. Zoo₂ predates on Zoo₁, and the change in the dynamics of Zoo₂ also
3 impacted the dynamics of Zoo₁, with a diminution of the maximum Zoo₁ C biomass
4 concentration. The *maximal grazing rate of nano-zooplankton* decrease also participated in this
5 change.

6 Two of the selected parameters shown in Table 3 correspond to the growth of bacteria. During
7 the optimisation procedure, the *net growth efficiency of bacteria* greatly increased from 0.3 to
8 0.99, whereas the *maximum uptake rate of bacteria* decreased from 4.25×10^{-5} to $1.97 \times 10^{-5} \text{ s}^{-1}$.
9 ¹. In our model, the growth of bacteria depended on the product of these two parameters. Finally,
10 this modification led to an increase in total bacterial growth in the ‘Control’ optimisation
11 compared to the initial simulation (see fig. 2-F). These two changes are antagonistic and highlight
12 the fact that the optimisation process modified combinations of parameters and not individual
13 parameters.

14 The decrease in the *maximal nitrification rate* from 5.91×10^{-7} to $2.52 \times 10^{-7} \text{ s}^{-1}$ contributed to
15 the diminution of nitrate concentration (fig. 2-A) in the ‘Control’ optimisation compared to the
16 initial simulation.

17 The *temperature coefficient for decomposition* increased from 2.95 to $4.35 \text{ }^\circ\text{C}^{-1}$, and the *reference*
18 *temperature for decomposition* greatly decreased. This change impacted the decomposition
19 process, which was temperature-dependent in our model. The decomposition process converts,
20 via the action of bacteria, non-living POM into DOM. The modification of these two parameters,
21 in addition to higher bacterial C biomass (fig. 2-F), led to an increase in DOC concentration (fig.
22 2-D). Decomposition and other temperature-dependent processes in the model (primary
23 production of phytoplankton, grazing by zooplankton, nitrification, etc.) were modified by the

1 optimisation procedure by changing the *reference temperature* and/or the *temperature coefficient*.
2 These two parameters acted as highly non-linear parameters.
3 The *internal quotas for Phy (N:C, P:C, and Si:C)* were also changed during the optimisation
4 process. The range of the (*Si:C*) *ratio* increased as the *maximal internal ratio* was changed from
5 0.19 to 0.38 mol Si mol C⁻¹. The phytoplankton community could thus consume more silicate to
6 build their skeleton or frustules (in the case of diatoms). From the initial simulation to the
7 ‘Control’ optimisation, the silicate concentration (fig. 2-C) decreased, becoming more similar to
8 the observations. The consumption of nitrate by the phytoplankton community varied less (see
9 fig. 2-A) because the interval length of (*N:C*) *quota* was reduced. Similarly, the interval length of
10 (*P:C*) *quota* increased, allowing more phosphate uptake by the phytoplankton community.
11 Several parameters presented a very large resolution, with a maximum of 0.78, but none of them
12 had a resolution equal to 1. Thus, a change in a single parameter value was not enough to adjust
13 our model. The optimisation procedure modified a linear combination of parameters.

14 **3.1.3 Analysis of data resolution**

15 The optimisation method allowed the calculation of data resolutions, which represent the
16 contribution of each observation as effective information to optimise the model. Fig. 7-A shows
17 data resolutions for the ‘Control’ optimisation, for the last iteration of the optimisation procedure.
18 The data resolution varied between sets of observations, which depended on sampling time.
19 Therefore, the data resolutions also varied during the experimental period.
20 Experimental observations of the Chl *a* concentration were effective information for the
21 optimisation procedure as they had the highest data resolution among the available observations.
22 The data resolution decreased from 1.00 on day 1 to 0.08 on day 4 and then reached 0.49 and

1 0.46 on days 5 and 6, respectively. At the end of the period, it remained below 0.25. The nitrate
2 data also had a high resolution at the very beginning and during the last few days of the
3 experiment. The phosphate data had increasing resolution throughout the experimental period,
4 from 0.06 initially to 0.31 at the end. The resolution of the silicate data followed the same trend
5 as that of the phosphate data, except on day 1, when the silicate data were more useful for the
6 optimisation process. The DOC data showed the same increase as the phosphate data. However,
7 on days 2, 3 and 4, the resolution of the DOC data was very low. The resolution of the bacterial
8 data decreased and varied between 0.71 and 0.09 during the experimental period.

9 On day 1, the Chl *a* and nitrate observations presented the highest resolutions for the optimisation
10 process. From day 2 to day 6, the Chl *a* and bacterial C biomass observations were the most
11 influential. During those 5 days, the resolution of other observations remained low in
12 comparison, except that of silicate on day 3. At the end of the period, the resolutions were almost
13 homogeneous among observations, even if the nitrate data had a relatively high resolution.

14 **3.2 ‘Oyster’ optimisation**

15 To estimate the best parameter values for the model including the new oyster compartment, an
16 optimisation procedure was performed with 180 parameters (166 initially and 14 added for
17 oysters). Realistic values for the new parameters were chosen according to the literature (see
18 Table 2). The initial filtration rate $filt_0$ was set to $2.31 \times 10^{-7} \text{ s}^{-1}$, as suggested by Chapelle et
19 al. (2000), and derived from Mazouni et al. (1996). The biodeposition rate $bd_{\%}$ was initially set
20 at 0.3 (Mazouni 1995). The filtration efficiency coefficients $effO_x$ were arbitrarily chosen (see
21 Table 2) but were free to change with the optimisation process, as were other parameters. As
22 previously mentioned, only one group of phytoplankton was considered, representing the entire

1 phytoplankton community. However, the model included three filtration efficiencies for
2 phytoplankton that can be used with three size classes of phytoplankton in future developments,
3 but two of them were useless for our study and were thus fixed at zero. Experimental
4 observations from mesocosms including oysters as top predators (Mostajir et al. 2015) were
5 assimilated. The first guess of the method included the 166 parameter values resulting from the
6 'Control' optimisation plus the 14 new parameter values, defined as the 'Oyster' initial
7 simulation. The optimisation process was iterated 75 times (i.e., 75×181 simulation runs). The
8 cost function ranged from 1.00 for the 'Oyster' initial simulation to 0.51 for the 'Oyster'
9 optimisation.

10 **3.2.1 Simulation results**

11 The nitrate concentration after optimisation was very similar to that in the observations (fig. 3-A).
12 The simulated mean value over the entire period was $0.108 \mu\text{M}$, compared to $0.104 \mu\text{M}$ for the
13 observations. Compared to the 'Control' optimisation (fig. 2-A), in the 'Oyster' optimisation, the
14 amplitude of the daily variations was low (fig. 3-A), and over the entire period, the concentration
15 ranged from a minimum of $0.07 \mu\text{M}$ to a maximum of $0.17 \mu\text{M}$.

16 Similarly, the phosphate concentration (fig. 3-B) of the 'Oyster' optimisation was more similar to
17 that of the observations than was the concentration in the 'Oyster' initial simulation. This
18 similarity was particularly pronounced for the second half of the experimental period, when the
19 concentration varied between 0.02 and $0.29 \mu\text{M}$. The daily variations occurring until day 3 were
20 relatively important compared with those on the following days.

21 The silicate concentration (fig. 3-C) in the optimised simulation was more similar to that of the
22 observations than the concentration in the initial simulation. The trend was also better than that in

1 the initial simulation. The silicate concentration decreased until day 3 and remained almost
2 constant thereafter, with a slight increase to 6.77 μM at the end of the experiment relative to the
3 concentration of 6.35 μM observed in the mesocosms.

4 With the addition of oysters, the ammonium concentration (fig. 8-A) exhibited an ever-increasing
5 trend in the 'Oyster' optimisation, varying from 1.20 μM in the 'Oyster' initial simulation to 2.73
6 μM in the optimised simulation on day 2. At the end, the simulated ammonium concentration was
7 10.91 μM .

8 The optimised simulated DOC concentration (fig. 3-D) showed a slight decrease and then
9 increased more than that in the 'Oyster' initial simulation to be more similar to that observed in
10 the mesocosms. However, the simulated concentrations were much lower than the observed
11 concentrations. The average DOC concentration over the entire period was 214.07 μM for the
12 optimised simulation and 261.73 μM for the observations.

13 From day 0 to day 2, the Chl *a* concentration (fig. 3-E) for the 'Oyster' optimisation exhibited the
14 same increase observed in the mesocosms, with an amplitude of daily variations of 1.2 mg m^{-3} .
15 Then, it decreased sharply on day 3 and periodically fluctuated thereafter. The maximum value in
16 the optimised simulation, reached on day 1, was 3.88 mg m^{-3} . Between day 5 and day 9, the
17 average concentration was 0.98 mg m^{-3} , compared to 0.20 mg m^{-3} for the observations.

18 The bacterial C biomass concentration (fig. 3-F) in the optimised simulation was more similar to
19 that for the observations than that in the initial simulation. It increased from day 0 until the end of
20 day 1, where it reached a maximum of 21.87 mmol C m^{-3} . Then, a quick decrease was simulated
21 until day 3. However, the simulated bacterial C biomass concentration remained lower than the
22 observed concentration from day 4 until the end of the experiment.

1 Concerning the zooplankton C biomass concentration (fig. 8-B), after day 3, Zoo₂ largely
2 dominated the zooplankton community. Its concentration reached a maximum of 25.00 mmol C
3 m⁻³ on day 3. The concentration in the optimised simulation followed a similar scheme as that in
4 the ‘Control’ simulation without oysters, with succession of domination by the different
5 zooplankton classes. However, the spikes appeared earlier in the simulation. The Zoo₃ C biomass
6 concentration was increased by the optimisation process. At the end of the experimental period,
7 the C biomass concentrations of Zoo₁, Zoo₂, and Zoo₃ were 1.88 mmol C m⁻³, 15.41 mmol C m⁻³,
8 and 2.34 mmol C m⁻³, respectively.

9 Fig. 9 shows the temporal evolution of oyster C biomass during the ten days of the experiment,
10 revealing a regular increase from the beginning until the end of the experiment of 9.2 to 16.5
11 mmol C m⁻³. The only information that we had at the beginning of the experiment was the
12 introduction of 10 oysters into each mesocosm. This initial condition was highly speculative, and
13 this led to careful consideration of the optimised value obtained for the filtration rate parameter
14 after optimisation. The adjustment of this initial condition for oyster C biomass should result in
15 an adjustment of oyster parameters.

16 **3.2.2 Analysis of adjusted parameters**

17 The optimisation procedure led to the calibration of the 180 parameters, including the new
18 parameters for oysters, as detailed in Table 2. Table 4 shows that the key parameters changed
19 during the optimisation according to their resolution. The new ‘Oyster’ parameters did not have
20 the highest resolution values (see Table 2). However, as expected, the *filtration rate* $filt_0$, the
21 *filtration efficiency of oysters for Phy* and the *biodeposition rate* $bd_{\%}$ changed very slightly
22 during the process.

1 Two of these key parameters concerned bacterial processes (Table 4). The *maximum uptake rate*
2 *for bacteria* greatly increased from 1.97 to $2.87 \times 10^{-5} \text{ s}^{-1}$, contributing to the increase in
3 bacterial C biomass concentration (fig. 3-F). Furthermore, DOM transformation into inorganic
4 nutrients greatly increased. The *bacterial (P:C) ratio* also changed during the optimisation
5 process, affecting the consumption of phosphate by bacteria.

6 Six key parameters concerned the processes of the phytoplankton community (Table 4). The
7 modification of two of them during optimisation affected the growth of the phytoplankton
8 community. First, the *maximal internal (Chl:N) ratio for Phy* increased, which resulted in a faster
9 increase in the Chl *a* concentration for the ‘Oyster’ optimisation than for the ‘Oyster’ initial
10 simulation. In contrast, the increase in the *half-saturation constant for nitrate uptake* from 2.24 to
11 $4.66 \mu\text{M}$ tended to decrease the growth of the phytoplankton community at a constant nitrate
12 concentration (fig. 3-A). These two changes had opposite effects, but the results showed higher
13 growth for Phy (fig. 3-E). This discrepancy could be related to the fact that the *maximal internal*
14 *(Chl:N) ratio* had a higher resolution value (0.84 against 0.38), i.e., higher importance in the
15 optimisation procedure. The *maximal (Si:C) ratio* also decreased, from 0.38 to 0.28 mol Si mol
16 C^{-1} . This modification caused the diminution of the silicate concentration after day 3 (fig. 3-C)
17 for the optimised simulation compared to the ‘Oyster’ initial simulation, even if the Chl *a*
18 concentration remained low (fig. 3-E).

19 In the same manner as in the ‘Control’ optimisation, seven parameters linked with zooplankton
20 processes are shown in Table 4. The parameters presented both a high resolution and a significant
21 change during the optimisation procedure and concerned different processes. For example, the
22 *maximal grazing rate of Zoo₂* and the *preference factor of Zoo₂ for bacteria* concerned predation

1 by zooplankton and thus their prey, whereas the *fraction of messy feeding for zooplankton*
2 concerned their messy feeding and thus light and heavy non-living POM concentrations.

3 **3.2.3 Analysis of data resolution**

4 In the ‘Oyster’ optimisation, the data resolution results were very different from those in the
5 ‘Control’ optimisation. According to fig. 7-B, on average, the phosphate and silicate data
6 resolutions were the highest, while the resolutions of the nitrate, Chl *a* and bacteria data were
7 almost equal. During the experimental period, the resolution for each observation showed
8 numerous variations.

9 The Chl *a* data resolution was high on days 1 and 3, at 0.53 and 0.84, respectively, but remained
10 low thereafter. The Chl *a* data resolution was the highest on day 4. The nitrate data resolution was
11 high on days 1, 3 and 7. It reached a maximum on day 7, at 0.99. The phosphate data resolution
12 was very high on days 2 and 3, reaching 0.98 on day 3. It was almost constant at approximately
13 0.25 during the last few days of the experiment. The silicate data resolution was also high on days
14 1, 7 and 9, when it reached a very high value of approximately 0.93. The DOC data resolution
15 remained very low during the experimental period, except on day 9, when it was 0.79. The DOC
16 data made the smallest contribution to the optimisation process. The bacterial data resolution was
17 higher on day 2, at 0.69, than on the other days of the experiment but made a good contribution to
18 the optimisation during the entire period of the experiment.

19 **4 Discussion**

20 To assess the impact of oysters as top predators on MFW dynamics, a modelling approach with
21 parameter optimisation was applied. The Eco3m-S biogeochemical model, coupled with the

1 optimisation method presented in section 2.3, efficiently reproduced observations made during a
2 mesocosm experiment. The optimisation method estimated a linear combination of parameters
3 giving the best compatibility with the six different observations (nitrate, phosphate, silicate,
4 DOC, Chl *a*, and bacterial C biomass). Finding a solution for the assimilation process is not a
5 simple curve-fitting procedure because of the complexity and non-linearity of the interactions
6 between the compartments of the model. Once the new biogeochemical model including oysters
7 was validated, the impact of oysters on the MFW was investigated by studying the structural
8 changes in the MFW and the interactions within the MFW.

9 **4.1 The potential of the parameter optimisation**

10 The parameter resolution resulting from the optimisation method reflected the importance of each
11 biogeochemical process in the model. Using this new benefit, the biogeochemical processes
12 could be sorted by importance. For example, in our modelling experiment, bacterial processes
13 played a very important role in MFW dynamics. Indeed, in both the ‘Control’ and ‘Oyster’
14 optimisations, the *maximum uptake rate for bacteria* exhibited the highest resolution of the entire
15 set of control parameters (see Table 3 and Table 4), in line with the major role played by bacteria
16 in the marine carbon cycle (e.g., Cho & Azam 1988, Azam et al. 1993).

17 In contrast, the low resolution of the control parameters of the new oyster compartment, with a
18 maximum of 0.08 (Table 2), showed that changing associated processes was not beneficial for the
19 optimisation process. However, the fact that parameter values did not change during the
20 optimisation might indicate that the choice of the initial values was robust and that these values
21 could thus be used for further studies.

1 To meet the mathematical requirements of the optimisation method, some of the most influential
2 parameters, i.e., those with the highest resolutions, were modified by optimisation and reached
3 unrealistic values. These unrealistic values allowed the simulated results to be more similar to the
4 experimental observations by minimising the cost function more efficiently. This was the case for
5 the *net growth efficiency for bacteria* and three other parameters controlling temperature
6 functions: the *reference temperature for zooplankton*, the *reference temperature for*
7 *decomposition*, and the *temperature coefficient for decomposition*. The optimisation method
8 preferred to change one parameter controlling the temperature functions, affecting several
9 temperature-dependent processes at the same time, over changing multiple parameters controlling
10 only one process each. Note that the parameters controlling temperature functions generally had a
11 high resolution value. Furthermore, unrealistic values could be explained with a deeper analysis
12 of other parameter values. According to the scientific literature, the *net growth efficiency for*
13 *bacteria* should be between 0.05 and 0.7 (Del Giorgio & Cole 1998). However, considering that
14 bacterial growth depends on the product of this parameter value with the value of the *maximal*
15 *uptake rate of bacteria*, the decrease in the *maximal uptake rate of bacteria* during the
16 optimisation process partially balanced the increase in the *net growth efficiency for bacteria*. For
17 example, for the ‘Control’ optimisation, the product varied from 1.28×10^{-5} to $1.95 \times 10^{-5} \text{ s}^{-1}$.
18 Indeed, the optimisation process modified a linear combination of parameters and not individual
19 parameters.

20 **4.2 Oysters induced structural changes in the MFW**

21 The introduction of oysters as top predators of the MFW led to a more heterotrophic ecosystem.
22 The structural autotroph:heterotroph C biomass ratio index (A:H, fig. 10) was calculated and
23 compared to results from Mostajir et al. (2015). This calculation was simple with the model,

1 which estimated the C biomass of each biological component of the model, in comparison with
2 experimental calculations, which were associated with strong uncertainties because of the C
3 biomass calculation method. The gap between the two simulations was less important than the
4 gaps associated with the experimental study, but the results were in the same direction. Overall,
5 the experimental MFW was well represented by the model, at least structurally, with only six
6 types of experimental observations assimilated. Therefore, the model corroborated the tendency
7 for a transition to a more heterotrophic MFW with the addition of oysters as top predators, which
8 could be useful for testing scenarios with the model. For example, the model could be used to
9 simulate a scenario with a higher quantity of oysters to assess the structural impact of more
10 intensive exploitation.

11 The main function of oysters in our model was filtering all mesocosm water containing living and
12 non-living organisms. Fig. 11 shows the filtration of each MFW component, resulting from
13 equation 10. According to the parameters used to define the filtration rate, the most filtrated
14 compartment corresponded to the phytoplankton community. Zooplankton was the second most
15 filtrated, and light non-living POM and bacteria were the third most filtrated. Our model included
16 the direct reduction of phytoplankton biomass by oysters by adding a new filtration term, $filt_{phy}$.
17 This result was in line with those of Cugier et al. (2010) and Mostajir et al. (2015). Nevertheless,
18 this process also indirectly impacted other components of the MFW, such as zooplankton, which
19 may find fewer prey in the phytoplankton community.

20 The simulated phytoplankton biomass was approximately 30% lower than the phytoplankton
21 biomass in the 'Control' optimisation (fig. 2-E versus 3-E). The bacterial biomass was also
22 affected, being 50% greater than that in the 'Control' optimisation (fig. 2-F versus 3-F). Oysters
23 strongly increased zooplankton biomass by approximately 110% (fig. 6-B versus 8-B). Therefore,

1 the increase in the biomass of zooplankton and reduction in the biomass of phytoplankton, which
2 are prey of zooplankton, could be in line with top-down control. The simulated predation of
3 phytoplankton by zooplankton was slightly higher in the ‘Oyster’ optimisation than in the
4 ‘Control’ optimisation (not shown), but this result does not fully explain the large increase in
5 zooplankton biomass. However, the reduction in phytoplankton biomass is explained by the top-
6 down control of oysters but also by the increased predation of zooplankton. Losey & Denno
7 (1998) showed that the combined influence of two predators could be greater than the sum of
8 their individual impacts. Here, the combined influence of oyster and zooplankton biomasses on
9 phytoplankton biomass was greater than the sum of the individual impacts.

10 The introduction of a top predator to an ecosystem could lead to unexpected results; in particular,
11 the introduction of an alien top predator could have a devastating impact on native species (e.g.,
12 Bytheway et al. 2016). In our case, we cannot exclude this possibility for the Thau lagoon
13 ecosystem, where non-native oysters (*Crassostrea gigas*, a Japanese oyster) have been cultivated
14 since 1972 (Hamon et al. 2003), because oysters exert strong structural control of the natural
15 lagoon MFW community.

16 **4.3 Indirect impact of oysters on bacterial biomass**

17 Simulated bacterial biomass strongly increased in the presence of oysters as top predators of the
18 MFW, in accordance with the study of Mostajir et al. (2015). Those authors proposed different
19 hypotheses to explain the increase in bacteria, and some of the hypotheses can be discussed based
20 on the new modelling results acquired here. First, bacteria might benefit from oyster excreta
21 (Mazouni et al. 1998), but as the excretion of oysters was not modelled in this study and
22 simulated bacterial biomass was similar to that in the experimental observations, this benefit

1 might not explain the increase. Second, Mostajir et al. (2015) highlighted the assumption that the
2 reduction in virus-like particles due to oyster filtration could favour an increase in bacterial
3 biomass. However, viruses were not modelled, particularly due to the complexity of their
4 interactions with other components of the MFW, and this assumption could not be investigated.

5 Our results support the third hypothesis posed by Mostajir et al. (2015), concerning the reduction
6 in competition between bacteria and phytoplankton for the uptake of nutrients. To quantify
7 competition between bacteria and phytoplankton, nutrient uptake fluxes were analysed. Fig. 12
8 shows the comparison between ‘Control’ and ‘Oyster’ optimisations for ammonium (fig. 12-A)
9 and phosphate uptake (fig. 12-B) by phytoplankton. For bacteria, the same comparison is shown
10 for ammonium uptake (fig. 12-C) and phosphate excretion (fig. 12-D). The model version of
11 Auger et al. (2011) includes potential control of bacterial growth by phosphorus availability, in
12 addition to limitation by carbon and nitrogen availability. This model formulation is derived from
13 Thingstad et al. (1998). Bacteria first absorb DOM, but they can also assimilate ammonium
14 and/or phosphate if DON and/or DOP are lacking. Bacteria can also act as decomposers and
15 excrete nutrients, depending on the comparison of DOC:DON and/or DOC:DOP with their
16 internal ratios (Kirchman et al. 2000). All the processes (nutrient uptake, excretion and
17 respiration) make the control of their stoichiometry possible. Our results showed that, except for
18 phosphate uptake, phytoplankton nutrient uptake was lower with the addition of oysters (fig. 12-
19 A and 12-B). Furthermore, in contrast to the pattern observed in the ‘Control’ optimisation,
20 where no ammonium bacterial uptake was observed (fig. 12-C), bacterial ammonium uptake
21 increased in the ‘Oyster’ optimisation after day 7. It can be concluded that competition between
22 bacteria and phytoplankton was reduced in our model, especially that for ammonium. In addition,
23 the excretion of phosphate by bacteria was higher with oysters and conveniently balanced the

1 higher phosphate needs of the phytoplankton community. Thingstad et al. (2007) showed that the
2 dynamics of a water column receiving nitrate, phosphate and DOC continuously shift to lower
3 nutrient competition and higher nutrient regeneration. The introduction of oysters slightly
4 increased the DOC, nitrate and phosphate concentrations in the water column, which could
5 correspond to the case studied by Thingstad et al. (2007).

6 Our results showed that the reduction in this competition benefited both bacterial and
7 phytoplankton growth. However, the phytoplankton community was subject to other strong
8 constraints, such as filtration by oysters, as explained above. Then, the larger quantity of nutrients
9 available for bacteria actually resulted in more bacterial biomass in the ‘Oyster’ simulation.

10 **4.4 Impact of oysters on the zooplankton community**

11 The increase in bacterial biomass in the ‘Oyster’ simulation favoured an increase in bacterivorous
12 zooplankton biomass (mainly Zoo₁ but also Zoo₂ in a smaller proportion). However, the Zoo₁ C
13 biomass slightly decreased with the addition of oysters (fig. 6-B versus 8-B). The maximum Zoo₁
14 C biomass of the ‘Oyster’ optimisation was 5.46 mmol C m⁻³ and was reached at the beginning of
15 day 2. On the same date, in the ‘Control’ simulation, the Zoo₁ C biomass was 4.41 mmol C m⁻³.
16 This result supports the idea that the increase in bacterial biomass favoured bacterivorous
17 zooplankton because the growth of Zoo₁ was higher in the presence of oysters.

18 The high Zoo₁ C biomass obtained in the presence of oysters led to a direct increase in the C
19 biomass of Zoo₂. Thus, Zoo₁ served as a link between bacteria and Zoo₂. Moreover, our results
20 showed an increase in Zoo₂ in the ‘Oyster’ simulation that was faster than the increase in Zoo₁
21 (fig. 8-B). Indeed, the predation pressure of Zoo₂ on Zoo₁ was higher than the predation pressure
22 of Zoo₁ on bacteria (not shown).

1 Therefore, in the presence of oysters, the phytoplankton community was greatly impacted by
2 direct oyster filtration. Furthermore, the reduction in competition between bacteria and
3 phytoplankton for the uptake of nutrients benefited bacteria and increased bacterial biomass. This
4 increase in bacterial biomass favoured bacterivorous zooplankton (Zoo_1), which were predated by
5 Zoo_2 . Finally, this phenomenon resulted in a higher Zoo_2 biomass in the ‘Oyster’ simulation than
6 in the ‘Control’ simulation. The modelling approach provided a real advantage in investigating
7 the interactions between different components of the MFW. The use of a mechanistic formulation
8 of biogeochemical processes (see section 2.2) renders the extraction of stocks and fluxes simple.
9 This discussion focused on filtration by oysters (fig. 11), predation by zooplankton and
10 competition between phytoplankton and bacteria for nutrients (fig. 12). These biogeochemical
11 fluxes, easily extracted from the simulation results, provided a great deal of new information for
12 our understanding of the impact of oysters as top predators of the MFW.

13 **5 Conclusion**

14 In this study, numerical ecosystem simulations with the Eco3m-S model were performed to
15 provide deeper insight into the interactions and fluxes within the MFW. A parameter optimisation
16 method assimilating mesocosm experimental observations described in Mostajir et al. (2015) was
17 used, and the model efficiently reproduced observations with and without oysters. The model
18 provided high-frequency results over the period of the experiment, and fluxes within the MFW
19 were extracted and analysed. For example, the comparison of nutrient uptakes by bacteria and the
20 phytoplankton community brought to light a decrease in competition for nutrients between these
21 two components of the MFW in the presence of oysters. Due to the filtration of all mesocosm
22 water including organisms and non-living particles, the direct and immediate impact of oysters

1 was mainly a reduction in phytoplankton carbon biomass. In addition, our results showed an
2 increase in zooplankton and bacterial biomasses. The mesocosms thus became more
3 heterotrophic with oysters. The reduction in competition for nutrients between bacteria and
4 phytoplankton, as mentioned above, resulted in a higher bacterial biomass in the ‘Oyster’
5 simulation. The increase in zooplankton biomass was explained by a strong increase in simulated
6 Zoo₂ biomass (50-200 µm, mainly ciliates and large flagellates) due to the grazing of Zoo₁
7 bacterivorous zooplankton (5-50 µm, mostly bacterivorous flagellates and small ciliates), which
8 appeared as an intermediary trophic link. In our study, oysters pushed the system to a more
9 heterotrophic state with higher micro-zooplankton and bacterial C biomasses and lower
10 phytoplankton C biomass.

11 Modelling, observation and experimentation are complementary for obtaining a good
12 understanding of ecological processes. Observation and experimentation provide a real but partial
13 view of the processes involved, and the ideal scenario in which everything could be observed or
14 monitored persists. Modelling approaches provide estimates more or less close to reality,
15 depending on the quality of known assumptions. However, such approaches often yield
16 information that is more complete and has a greater temporal resolution. Models are fed with
17 theories and observations. The modelling approach introduces a new point of view, which is
18 useful for understanding biogeochemical mechanisms, paying attention to assumptions made
19 beforehand. In our case, we succeeded in reproducing not only the steady state of the observed
20 mesocosm experiment but also the dynamics of the ecosystem over the 10 days of the
21 experimental period. Additional information was provided by the model, such as biogeochemical
22 fluxes within the MFW. This idea could encourage the scientific community to pursue more
23 interactions between modelling, observations and experimental communities.

1 Analysing the data assimilated during the optimisation process could also be a simple way to
2 define the most interesting data required for the modelling approach. It could help manage
3 experimental efforts in order to conduct a more realistic modelling study. For example, in our
4 study, data available for Chl *a* or bacteria were very important for the ‘Control’ optimisation.
5 Furthermore, our results were very similar to mesocosm observations and suggested that
6 ammonium observations, which were not available, were not essential in this specific case. Data
7 resolutions also contain temporal information that reveals, for example, if it is better to measure
8 each variable once a day or measure one variable at a high frequency and others at a low
9 frequency. The answer strongly depends on the system’s dynamics and the complexity of the
10 processes involved. Regarding our results, a good effort to obtain numerous Chl *a* observations is
11 needed, compared to DOC observations, which could be measured only once a week for example.

12 **Acknowledgements**

13 This work was supported by the CNRS-INSU project “CHIFRE” and a PhD grant from the
14 Montpellier University. We also thank the “American Journal Expert” company for reviewing the
15 English.

16 **References**

17 Auger PA, Diaz F, Ulses C, Estournel C, Neveux J, Joux F, Pujo-Pay M, Naudin JJ (2011)
18 Functioning of the planktonic ecosystem on the Gulf of Lions shelf (NW Mediterranean) during
19 spring and its impact on the carbon deposition: a field data and 3-D modelling combined
20 approach. *Biogeosciences* 8:3231–3261.

- 1 Auger PA, Ulses C, Estournel C, Stemmann L, Somot S, Diaz F (2014) Interannual control of
2 plankton communities by deep winter mixing and prey/predator interactions in the NW
3 Mediterranean: Results from a 30-year 3D modeling study. *Progress in Oceanography* 124:12–
4 27.
- 5 Azam F, Smith DC, Steward GF, Hagström Å. (1993) Bacteria-organic matter coupling and its
6 significance for oceanic carbon cycling. *Microb Ecol* 28:167–179.
- 7 Barillé L, Prou J, Héral M, Bourgrier S (1993) No influence of food quality, but ration-dependent
8 retention efficiencies in the Japanese oyster *Crassostrea gigas*. *Journal of Experimental Marine*
9 *Biology and Ecology* 171:91–106.
- 10 Bayne BL (2017) Feeding. In: Osborn P (ed) *Biology of oysters. Developments in aquaculture*
11 *and fisheries science*, vol 41. Academic Press, London/San Diego.
- 12 Bytheway JP, Price CJ, Banks PB (2016) Deadly intentions: naïve introduced foxes show rapid
13 attraction to odour cues of an unfamiliar native prey. *Scientific Reports* 6.
- 14 Callier M, Weise A, McKindsey C, Desrosiers G (2006) Sedimentation rates in a suspended
15 mussel farm (Great-Entry Lagoon, Canada): biodeposit production and dispersion. *Mar Ecol Prog*
16 *Ser* 322:129–141.
- 17 Callier MD, Richard M, McKindsey CW, Archambault P, Desrosiers G (2009) Responses of
18 benthic macrofauna and biogeochemical fluxes to various levels of mussel biodeposition: An in
19 situ “benthocosm” experiment. *Marine Pollution Bulletin* 58:1544–1553.

- 1 Chapelle A, Ménesguen A, Deslous-Paoli J-M, Souchu P, Mazouni N, Vaquer A, Millet B (2000)
2 Modelling nitrogen, primary production and oxygen in a Mediterranean lagoon. Impact of oysters
3 farming and inputs from the watershed. *Ecological modelling* 127:161–181.
- 4 Cho BC, Azam F (1988) Major role of bacteria in biogeochemical fluxes in the ocean's interior.
5 *Nature* 332:441–443.
- 6 Cugier P, Struski C, Blanchard M, Mazurié J, Pouvreau S, Olivier F, Trigui JR, Thiébaud E
7 (2010) Assessing the role of benthic filter feeders on phytoplankton production in a shellfish
8 farming site: Mont Saint Michel Bay, France. *Journal of Marine Systems* 82:21–34.
- 9 De Crignis M (2007) Sources de nourriture et bio-énergétique de l'huître creuse *Crassostrea gigas*
10 : les nanoflagellés et les ciliés jouent-ils un rôle dans le budget d'énergie dynamique d'huîtres.
11 MSc dissertation. Université de La Rochelle, La Rochelle, France.
- 12 Defossez J-M, Hawkins AJS (1997) Selective feeding in shellfish: size-dependent rejection of
13 large particles within pseudofaeces from *Mytilus edulis*, *Ruditapes philippinarum* and *Tapes*
14 *decussatus*. *Marine Biology* 129:139–147.
- 15 Duarte P, Meneses R, Hawkins AJS, Zhu M, Fang J, Grant J (2003) Mathematical modelling to
16 assess the carrying capacity for multi-species culture within coastal waters. *Ecological Modelling*
17 168:109–143.
- 18 Dupuy C, Le Gall S, Hartmann H, Bréret M (1999) Retention of ciliates and flagellates by the
19 oyster *Crassostrea gigas* in French Atlantic coastal ponds: protists as a trophic link between
20 bacterioplankton and benthic suspension-feeders. *Mar Ecol Prog Ser* 177:165–175.

1 Dupuy C, Vaquer A, Lam-Höai T, Rougier C, Mazouni N, Lautier J, Collos Y, Le Gall S (2000)
2 Feeding rate of the oyster *Crassostrea gigas* in a natural planktonic community of the
3 Mediterranean Thau Lagoon. *Marine Ecology Progress Series* 205:171–184.

4 Frikha MG, Linley EAS, Delmas D (1987) Evolution annuelle et saisonnière de la microbiomasse
5 d'une claire à huîtres : importance des populations bactérioplanctoniques. *Oceanis* 13:433–447.

6 Froján M, Arbones B, Zúñiga D, Castro CG, Figueiras FG (2014) Microbial plankton community
7 in the Ría de Vigo (NW Iberian upwelling system): impact of the culture of *Mytilus*
8 galloprovincialis. *Marine Ecology Progress Series* 498:43–54.

9 Gangnery A, Bacher C, Buestel D (2001) Assessing the production and the impact of cultivated
10 oysters in the Thau lagoon (Mediterranee, France) with a population dynamics model. *Can J Fish*
11 *Aquat Sci* 58:1012–1020.

12 Gangnery A, Chabirand J-M, Lagarde F, Le Gall P, Oheix J, Bacher C, Buestel D (2003) Growth
13 model of the Pacific oyster, *Crassostrea gigas*, cultured in Thau Lagoon (Méditerranée, France).
14 *Aquaculture* 215:267–290.

15 Gangnery A, Bacher C, Buestel D (2004) Modelling oyster population dynamics in a
16 Mediterranean coastal lagoon (Thau, France): sensitivity of marketable production to
17 environmental conditions. *Aquaculture* 230:323–347.

18 Del Giorgio PA, Cole JJ (1998) Bacterial growth efficiency in natural aquatic systems. *Annual*
19 *Review of Ecology and Systematics* 29:503–541.

20 Gonzalez Vicente P (1986) Recherche de la dimension de l'espace latent en ACP. *Statistique et*
21 *Analyse des données* 11:19–29.

- 1 Gosling E (2015) How bivalves feed. In: *Marine Bivalve Molluscs*. John Wiley & Sons,
2 Chichester, UK, p 99–156.
- 3 Grant J, Bacher C, Cranford PJ, Guyonnet T, Carreau M (2008) A spatially explicit ecosystem
4 model of seston depletion in dense mussel culture. *Journal of Marine Systems* 73:155–168.
- 5 Hamon P-Y, Vercelli C, Pichot Y, Lagarde F, Le Gall P, Oheix J (2003) Les malaïgues de l'étang
6 de Thau. Tome 1. Description des malaïgues. Moyens de lutte, Recommandations. Archives
7 Ifremer.
- 8 Haven DS, Morales-Alamo R (1966) Aspects of biodeposition by oysters and other invertebrate
9 filter feeders. *Limnol Oceanogr* 11:487–498.
- 10 Ibarra DA, Fennel K, Cullen JJ (2014) Coupling 3-D Eulerian bio-physics (ROMS) with
11 individual-based shellfish ecophysiology (SHELL-E): A hybrid model for carrying capacity and
12 environmental impacts of bivalve aquaculture. *Ecological Modelling* 273:63–78.
- 13 Jansen H, Strand Ø, Strohmeier T, Krogness C, Verdegem M, Smaal A (2011) Seasonal
14 variability in nutrient regeneration by mussel *Mytilus edulis* rope culture in oligotrophic systems.
15 *Mar Ecol Prog Ser* 431:137–149.
- 16 Kirchman DL, Meon B, Cottrell MT, Hutchins DA, Weeks D, Bruland KW (2000) Carbon versus
17 iron limitation of bacterial growth in the California upwelling regime. *Limnol Oceanogr*
18 45:1681–1688.
- 19 Kooijman SALM (1986) Energy budgets can explain body size relations. *Journal of Theoretical*
20 *Biology* 121:269–282.

- 1 Kooijman SALM (2000) *Dynamic Energy and Mass Budgets in Biological Systems*, 2nd ed.
2 Cambridge University Press, Cambridge.
- 3 Kooijman B (2009) *Dynamic Energy Budget Theory for Metabolic Organisation*, 3rd ed.
4 Cambridge University Press, Cambridge.
- 5 Le Gall J-L, Raillard O (1988) Influence de la température sur la physiologie de l'huître
6 *Crassostrea gigas*. *Océanis* 14:603–608.
- 7 Le Gall S, Hassen M, Le Gall P (1997) Ingestion of a bacterivorous ciliate by the oyster
8 *Crassostrea gigas*: protozoa as a trophic link between picoplankton and benthic suspension-
9 feeders. *Marine Ecology Progress Series* 152:301–306.
- 10 Losey JE, Denno RF (1998) Positive predator-predator interactions: enhanced predation rates and
11 synergistic suppression of aphid populations. *Ecology* 79:2143–2152.
- 12 Marinov D, Galbiati L, Giordani G, Viaroli P, Norro A, Bencivelli S, Zaldívar J-M (2007) An
13 integrated modelling approach for the management of clam farming in coastal lagoons.
14 *Aquaculture* 269:306–320.
- 15 Mazouni N (1995) Influence des élevages ostréicoles sur le fonctionnement d'un écosystème
16 lagunaire méditerranéen. Etude in situ de l'influence des filtreurs (coquillages et épibiontes) sur
17 les flux de matières particulaire et dissoute. PhD dissertation. Université Aix-Marseille II,
18 Marseille, France.
- 19 Mazouni N, Gaertner J-C, Deslous-Paoli J-M, Landrein S, Geringer d'Oedenberg M (1996)
20 Nutrient and oxygen exchanges at the water-sediment interface in a shellfish farming lagoon
21 (Thau, France). *Journal of Experimental Marine Biology and Ecology* 205:91–113.

- 1 Mazouni N, Gaertner J-C, Deslous-Paoli J-M (1998) Influence of oyster culture on water column
2 characteristics in a coastal lagoon (Thau, France). In: Oceans, Rivers and Lakes: Energy and
3 Substance Transfers at Interfaces. Amiard J-C, Le Rouzic B, Berthet B, Bertru G (eds) Springer
4 Netherlands, Dordrecht, p 149–156.
- 5 Mazouni N (2004) Influence of suspended oyster cultures on nitrogen regeneration in a coastal
6 lagoon (Thau, France). *Mar Ecol Prog Ser* 276:103–113.
- 7 Mostajir B, Roques C, Bouvier C, Bouvier T, Fouilland É, Got P, Le Floc’h E, Nouguié J, Mas
8 S, Sempéré R (2015) Microbial food web structural and functional responses to oyster and fish as
9 top predators. *Marine Ecology Progress Series* 535:11–27.
- 10 Plus M, Auby I, Maurer D, Trut G, Del Amo Y, Dumas F, Thouvenin B (2015) Phytoplankton
11 versus macrophyte contribution to primary production and biogeochemical cycles of a coastal
12 mesotidal system. A modelling approach. *Estuarine, Coastal and Shelf Science* 165:52–60.
- 13 Prunet P, Minster J-F, Ruiz-Pino D, Dadou I (1996) Assimilation of surface data in one-
14 dimensional physical-biogeochemical model of the surface ocean. 1. Method and preliminary
15 results. *Global biogeochemical cycles* 10:111–138.
- 16 Richard M, Archambault P, Thouzeau G, McKindsey CW, Desrosiers G (2007) Influence of
17 suspended scallop cages and mussel lines on pelagic and benthic biogeochemical fluxes in Havre-
18 aux-Maisons Lagoon, Îles-de-la-Madeleine (Quebec, Canada). *Can J Fish Aquat Sci* 64:1491–
19 1505.
- 20 Richard M, Bec B, Vanhuyse C, Mas S, Parin D, Chantalat C, Le Gall P, Fiandrino A, Lagarde
21 F, Mortreux S, Ouisse V, Rolland JL, Degut A, Hatey E, Fortune M, Roque d’Orbcastel E,
22 Messiaen G, Munaron D, Callier M, Oheix J, Derolez V, Mostajir B (2019) Changes in

1 planktonic microbial components in interaction with juvenile oysters during a mortality episode
2 in the Thau lagoon (France). *Aquaculture* 503:231–241.

3 Robert P, Mckindsey CW, Chaillou G, Archambault P (2013) Dose-dependent response of a
4 benthic system to biodeposition from suspended blue mussel (*Mytilus edulis*) culture. *Marine*
5 *Pollution Bulletin* 66:92–104.

6 Sherman E, Moore JK, Primeau F, Tanouye D (2016) Temperature influence on phytoplankton
7 community growth rates. *Global Biogeochem Cycles* 30:550–559.

8 Sime-Ngando T, Gosselin M, Roy S, Chanut J-P (1995) Significance of planktonic ciliated
9 protozoa in the Lower St. Lawrence Estuary: comparison with bacterial, phytoplankton, and
10 particulate organic carbon. *Aquatic Microbial Ecology* 9:243-258.

11 Souchu P, Vaquer A, Collos Y, Landrein S, Deslous-Paoli J, Bibent B (2001) Influence of
12 shellfish farming activities on the biogeochemical composition of the water column in Thau
13 lagoon. *Mar Ecol Prog Ser* 218:141–152.

14 Spillman CM, Hamilton DP, Hipsey MR, Imberger J (2008) A spatially resolved model of
15 seasonal variations in phytoplankton and clam (*Tapes philippinarum*) biomass in Barbamarco
16 Lagoon, Italy. *Estuarine, Coastal and Shelf Science* 79:187–203.

17 Thingstad TF, Havskum H, Zweifel UL, Berdalet E, Sala MM, Peters F, Alcaraz M, Scharek R,
18 Perez M, Jacquet S, Flaten GAF, Dolan JR, Marrasé C, Rassoulzadegan F, Hagstrøm Å, Vaultot
19 D (2007) Ability of a “minimum” microbial food web model to reproduce response patterns
20 observed in mesocosms manipulated with N and P, glucose, and Si. *Journal of Marine Systems*
21 64:15–34.

- 1 Thingstad TF, Zweifel UL, Rassoulzadegan F (1998) P limitation of heterotrophic bacteria and
 2 phytoplankton in the northwest Mediterranean. *Limnol Oceanogr* 43:88–94.
- 3 Trottet A, Roy S, Tamigneaux E, Lovejoy C, Tremblay R (2008) Impact of suspended mussels
 4 (*Mytilus edulis* L.) on plankton communities in a Magdalen Islands lagoon (Québec, Canada): A
 5 mesocosm approach. *Journal of Experimental Marine Biology and Ecology* 365:103–115.
- 6 Ulses C, Auger P-A, Soetaert K, Marsaleix P, Diaz F, Coppola L, Herrmann MJ, Kessouri F,
 7 Estournel C (2016) Budget of organic carbon in the North-Western Mediterranean open sea over
 8 the period 2004-2008 using 3-D coupled physical-biogeochemical modeling. *J Geophys Res*
 9 *Oceans* 121:7026–7055.
- 10 Vidussi F, Mostajir B, Fouilland E, Le Floc’h E, Nougulier J, Roques C, Got P, Thibault-Botha D,
 11 Bouvier T, Troussellier M (2011) Effects of experimental warming and increased ultraviolet B
 12 radiation on the Mediterranean plankton food web. *Limnology and Oceanography* 56:206–218.
- 13 Wunsch C (1978) The North Atlantic general circulation west of 50°W determined by inverse
 14 methods. *Reviews of Geophysics* 16:583–620.
- 15 Zaldívar JM, Cattaneo E, Plus M, Murray CN, Giordani G, Viaroli P (2003) Long-term
 16 simulation of main biogeochemical events in a coastal lagoon: Sacca Di Goro (Northern Adriatic
 17 Coast, Italy). *Continental Shelf Research* 23:1847–1875.

18 **Tables**

19 *Table 1: List of state variables in the Eco3m-S model.*

State variables	Description	Unit
NO ₃ , NH ₄ , PO ₄ , SiO ₄	Nitrate, phosphate, ammonium, silicate	mmol m ⁻³

XPhy	Phytoplankton community in X, with X corresponding to carbon (C), nitrogen (N), phosphorus (P), or silica (Si)	mmol X m ⁻³
ChlPhy	Phytoplankton in chlorophyll	mg Chl m ⁻³
CZoo ₁ , CZoo ₂ , CZoo ₃	Zooplankton C biomass	mmol C m ⁻³
CBac	Bacterial C biomass	mmol C m ⁻³
DOX	Dissolved organic X, with X = carbon, nitrogen, phosphorus, or silica	mmol X m ⁻³
nl-POX _y	Heavy (y = h) and light (y = l) non-living particulate organic X (organic detritus), with X = carbon, nitrogen, phosphorus, or silica	mmol X m ⁻³
ChlDet	Light chlorophyll detritus coming from phytoplankton death or egestion of zooplankton	mg Chl m ⁻³

1
2 *Table 2: List of the new parameters for oysters introduced to the Eco3m-S model. (1) Chapelle et*
3 *al. (2000), (2) Le Gall et al. (1997), (3) Defossez et Hawkins (1997), (4) De Crignis (2007) (5)*
4 *Dupuy et al. (2000), (6) Grant et al. (2008), (7) Mazouni (1995), (8) Le Gall et Raillard (1988).*

Name		Initial value	Final Value	Units	Resolution
Maximal filtration rate ¹	$filt_0$	2.31×10^{-7}	2.02×10^{-7}	s ⁻¹	0.05
Filtration efficiency on Zoo ₃	$effO_{Zoo3}$	0.00	0.00	-	0.00
Filtration efficiency on Zoo ₂ ^{2,3,4,5}	$effO_{Zoo2}$	0.10	0.10	-	0.00
Filtration efficiency on Zoo ₁ ^{2,3,4,5}	$effO_{Zoo1}$	0.15	0.15	-	0.00
Filtration efficiency on Phy ₃ ^{2,4,5}	$effO_{Phy3}$	0.50	0.45	-	0.02
Filtration efficiency on Phy ₂	$effO_{Phy2}$	0.00	0.00	-	0.00
Filtration efficiency on Phy ₁	$effO_{Phy1}$	0.00	0.00	-	0.00
Filtration efficiency on bacteria ^{2,4}	$effO_{Bact}$	0.05	0.05	-	0.00
Filtration efficiency on light non-living POM ^{2,6}	$effO_{lDet}$	0.10	0.10	-	0.00
Filtration efficiency on heavy non-living POM ^{2,6}	$effO_{hDet}$	0.10	0.10	-	0.00
Biodeposition rate ⁷	$bd_{\%}$	0.30	0.34	-	0.02
Rate of light non-living POM in biodeposits (with the rest being heavy)	k_{Det}	0.50	0.48	-	0.01
Temperature coefficient for the oyster temperature function ¹	Q_{10}^{oyster}	2.00	2.02	°C ⁻¹	0.00

Reference temperature for oysters ^{1,8} T_{ref}^{oyster} 18.00 21.07 °C 0.08

1
2 *Table 3: The list of key parameters changed during the ‘Control’ optimisation process*
3 *assimilating ‘Control’ mesocosm observations.*

Name	Initial value	Final Value	Units	Resolution
Maximum uptake rate of bacteria	4.25×10^{-5}	1.97×10^{-5}	s ⁻¹	0.78
Maximal Chl:N ratio of Phy	2.30	2.03	mg Chl mmol N ⁻¹	0.77
Reference temperature for zooplankton processes	18.00	12.50	°C	0.64
Maximal internal Si:C ratio of Phy	0.19	0.38	mol Si mol C ⁻¹	0.58
Maximal internal N:C quota of Phy	0.20	0.19	mol N mol C ⁻¹	0.54
Preference factor of Zoo ₂ for Zoo ₁	0.25	0.41	-	0.49
Half-saturation constant for nitrate uptake for Phy	1.00	2.24	mmol N m ⁻³	0.49
Maximal grazing rate of Zoo ₁ at 15.5 °C	4.50×10^{-5}	3.68×10^{-5}	s ⁻¹	0.40
Net growth efficiency of zooplankton	0.80	0.75	-	0.38
Maximal grazing rate of Zoo ₂ at 15.5 °C	3.00×10^{-5}	5.60×10^{-5}	s ⁻¹	0.37
Net growth efficiency of bacteria	0.30	0.99	-	0.36
Maximal internal P:C quota of Phy	1.90×10^{-2}	2.85×10^{-2}	mol P mol C ⁻¹	0.34
Preference factor of Zoo ₂ for Phy	0.15	0.06	-	0.29
Reference temperature for decomposition processes	20.00	9.37	°C	0.28
Fraction of messy feeding for zooplankton	0.23	0.31	-	0.27
Maximal nitrification rate at 0°C	5.91×10^{-7}	2.52×10^{-7}	s ⁻¹	0.17
Temperature coefficient for decomposition	2.95	4.35	°C ⁻¹	0.16

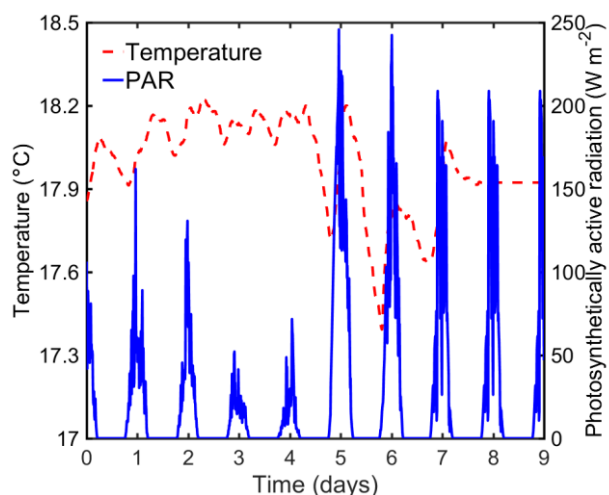
4
5 *Table 4: The list of key parameters changed during the ‘Oyster’ optimisation process*
6 *assimilating ‘Oyster’ mesocosm observations.*

Name	Initial value	Final Value	Units	Resolution
Maximum uptake rate of bacteria	1.97×10^{-5}	2.87×10^{-5}	s ⁻¹	0.84
Maximal internal Si:C ratio of Phy	0.38	0.28	mol Si mol C ⁻¹	0.63

Maximal internal Chl:N ratio of Phy	2.03	2.24	mg Chl mmol N ⁻¹	0.51
Reference temperature for zooplankton processes	12.50	11.52	°C	0.49
Ratio of small/large organic matter in dead zooplankton	0.99	1.09	-	0.48
Fraction of messy feeding for zooplankton	0.31	0.27	-	0.42
Maximal internal N:C ratio of Phy	0.19	0.13	mol N mol C ⁻¹	0.40
P:C ratio of bacteria	0.94×10^{-2}	1.32×10^{-2}	mol P mol C ⁻¹	0.38
Ratio of small/large particulate organic matter in dead Phy	0.82	0.87	-	0.36
Maximal grazing rate of Zoo ₂ at 15.5 °C	5.60×10^{-5}	5.49×10^{-5}	s ⁻¹	0.32
Preference factor of Zoo ₂ for bacteria	6.98×10^{-2}	6.18×10^{-2}	-	0.31
Half-saturation constant for nitrate uptake for Phy	2.24	4.66	mmol N m ⁻³	0.30
Fixed P:C ratio of Zoo ₂	1.44×10^{-2}	1.51×10^{-2}	mol P mol C ⁻¹	0.30
Maximal internal P:C ratio of Phy	2.85×10^{-2}	3.55×10^{-2}	mol P mol C ⁻¹	0.27
Fixed N:C ratio of Zoo ₂	0.19	0.14	mol N mol C ⁻¹	0.24

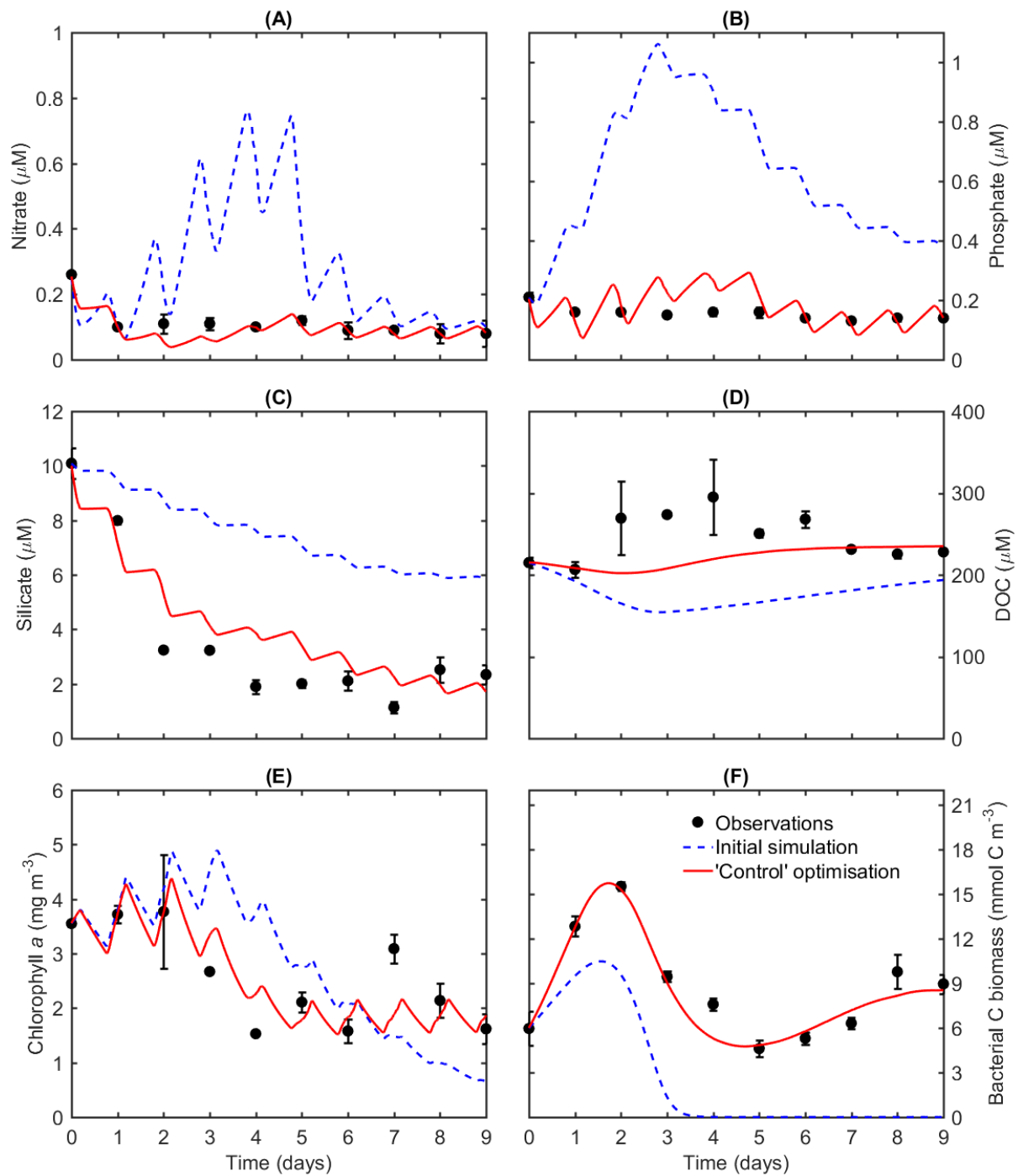
1

2 Figures



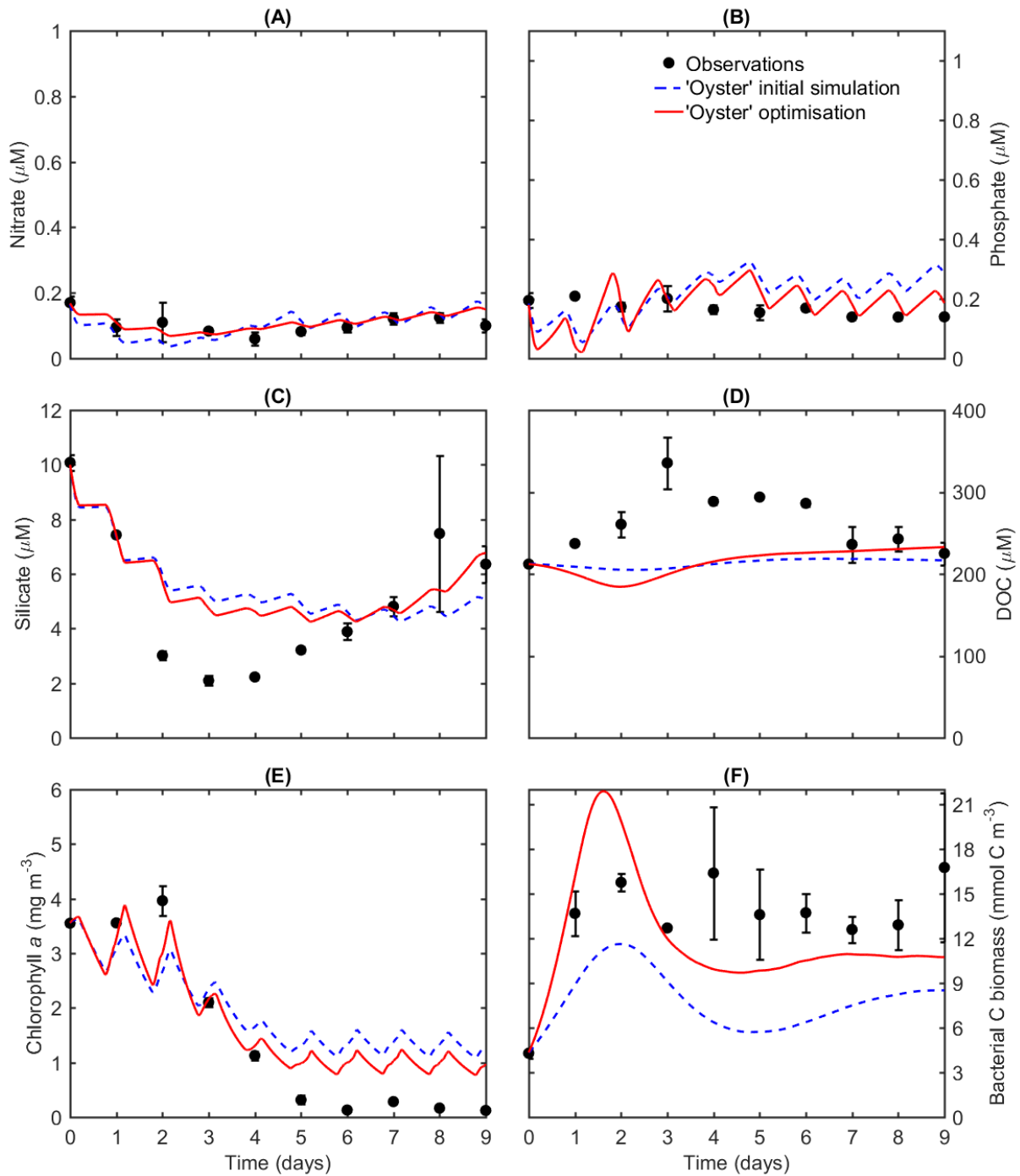
3

4 *Figure 1: Temperature (°C, red) and photosynthetically active radiation (PAR, W m⁻², blue)*
5 *measured during the mesocosm experimental study and used to force the biogeochemical model.*



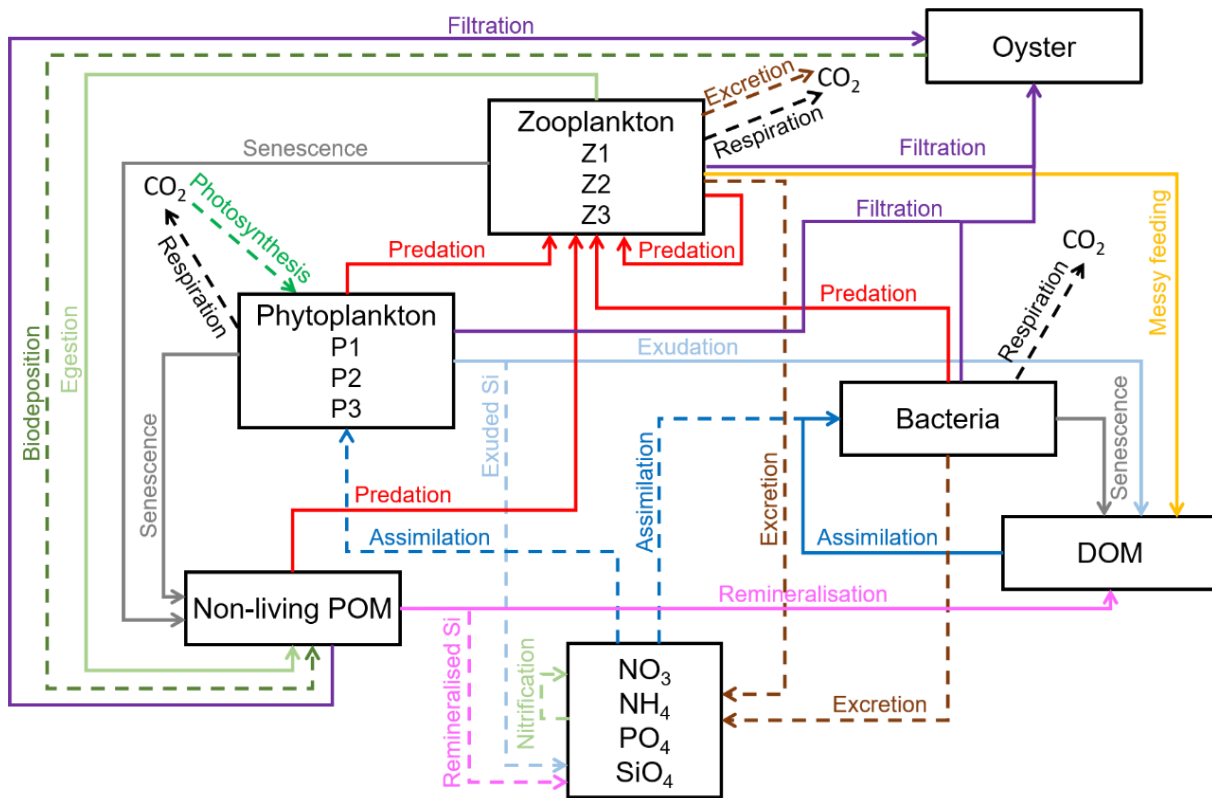
1
 2 *Figure 2: Comparison among the mesocosm experimental study (black circles), initial simulation*
 3 *(blue dashed line), and 'Control' optimisation (red line) for the (A) nitrate concentration (μM),*
 4 *(B) phosphate concentration (μM), (C) silicate concentration (μM), (D) dissolved organic carbon*

1 concentration (μM), (E) chlorophyll *a* concentration (mg m^{-3}), and (F) bacterial C biomass
 2 concentration (mmol C m^{-3}).

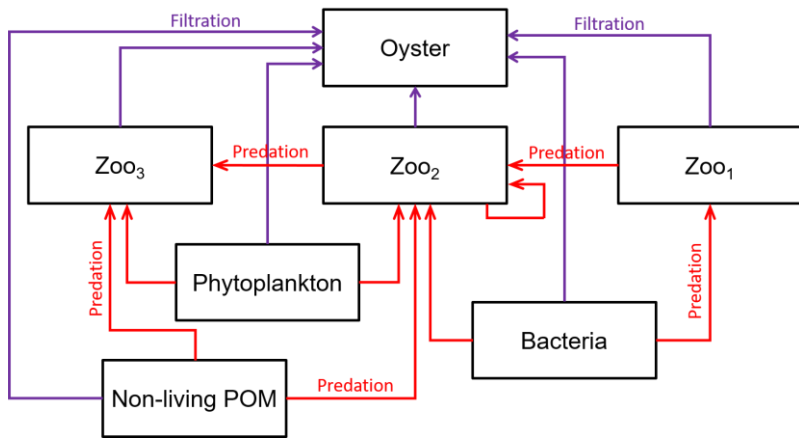


3
 4 *Figure 3: Comparison among the mesocosm experimental study (black circles), 'Oyster' initial*
 5 *simulation (blue dashed line), and 'Oyster' optimisation (red line) for the (A) nitrate*
 6 *concentration (μM), (B) phosphate concentration (μM), (C) silicate concentration (μM), (D)*

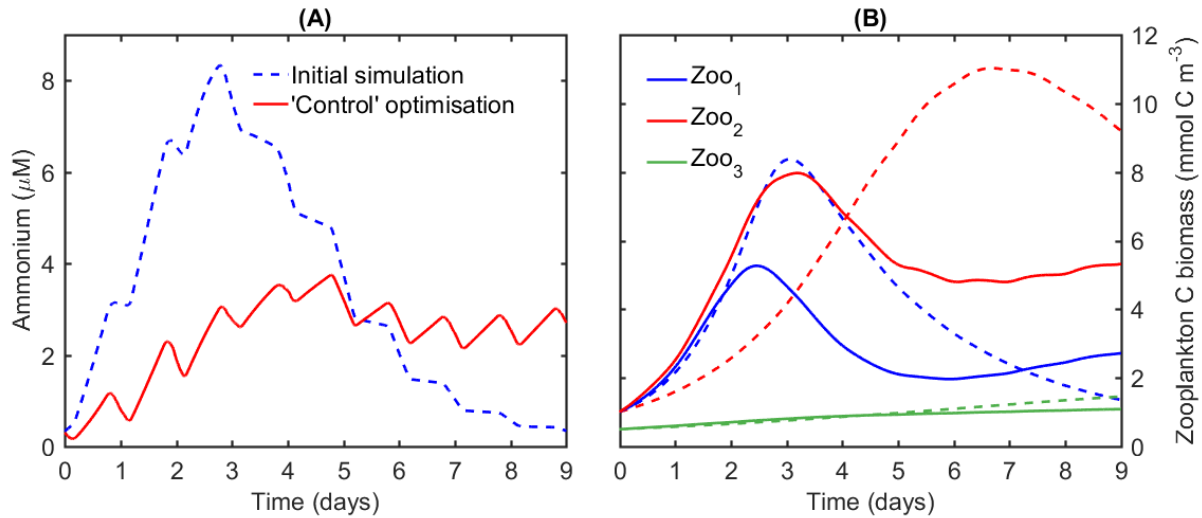
- 1 dissolved organic carbon concentration (μM), (E) chlorophyll a concentration (mg m^{-3}), and (F)
 2 bacterial C biomass concentration (mmol C m^{-3}).



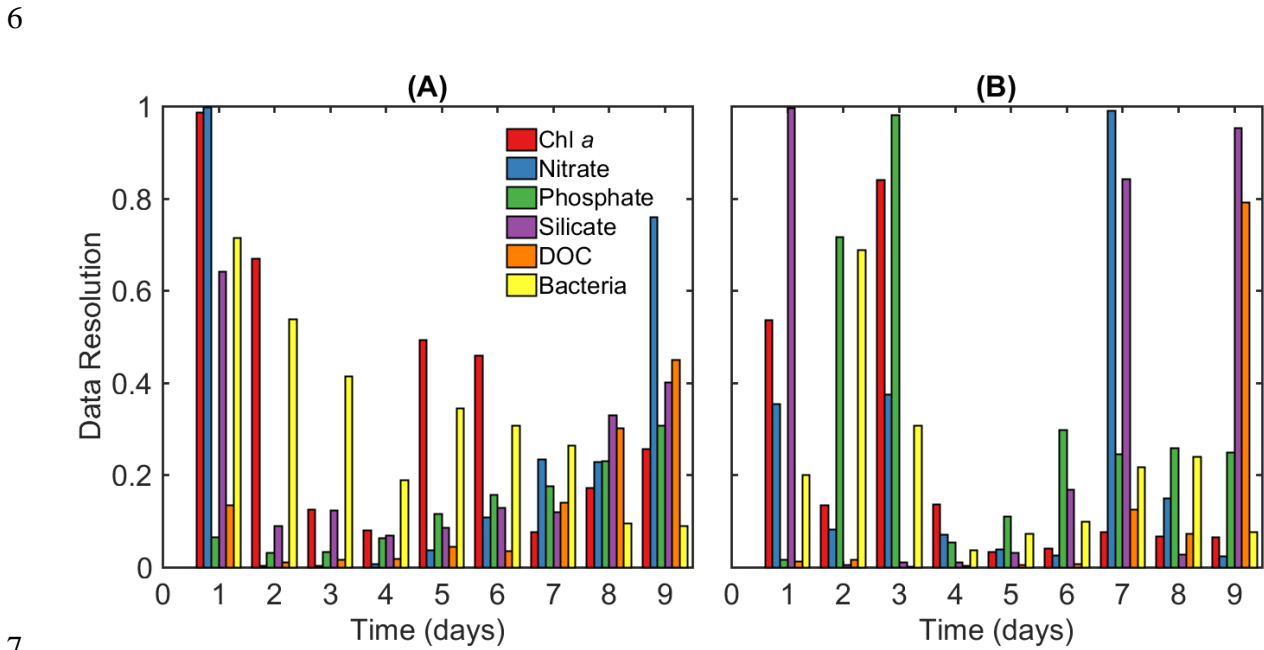
3
 4 Figure 4: Diagram of the Eco3m-S ecosystem model with the main functional groups,
 5 biochemical constituents and processes. A new compartment for oysters was introduced. Adapted
 6 from Auger et al. (2011).



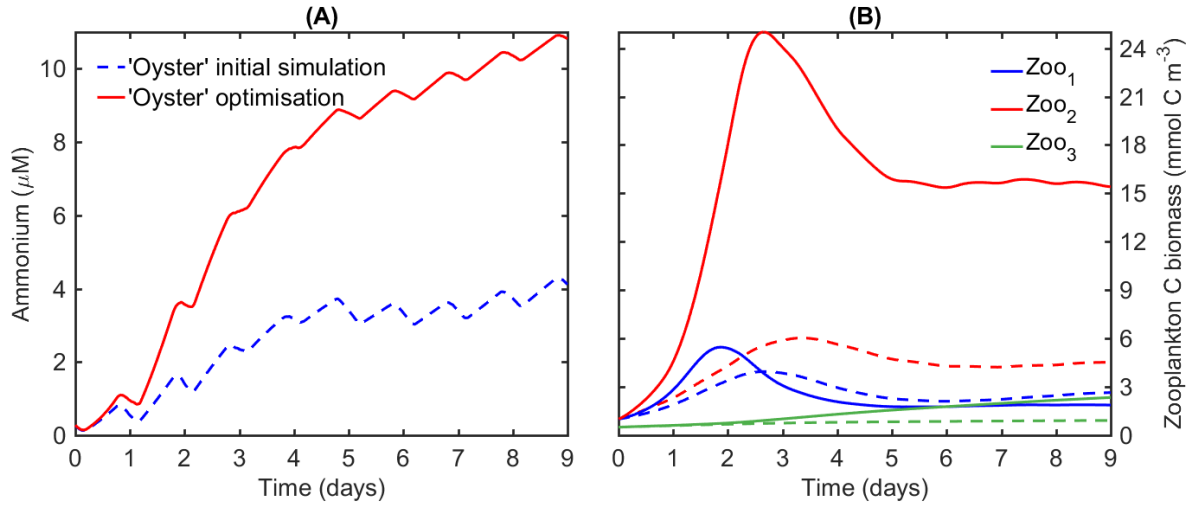
7
 8 Figure 5: Schematic view of the predation (red) and filtration (purple) links in the model in the
 9 presence of oysters.



1
 2 *Figure 6: Comparison between the initial simulation (dashed lines) and 'Control' optimisation*
 3 *(solid lines) for the (A) ammonium concentration (μM) and (B) zooplankton C biomass*
 4 *concentration (mmol C m^{-3}). The three compartments of zooplankton are represented: Zoo₁*
 5 *(blue), Zoo₂ (red), and Zoo₃ (green).*

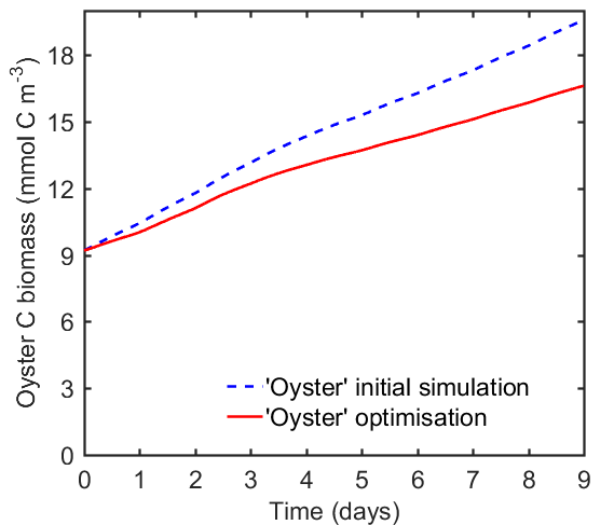


7
 8 *Figure 7: Data resolution for each type of observation, detailed for each day of the experiment,*
 9 *for the (A) 'Control' optimisation and (B) 'Oyster' optimisation.*

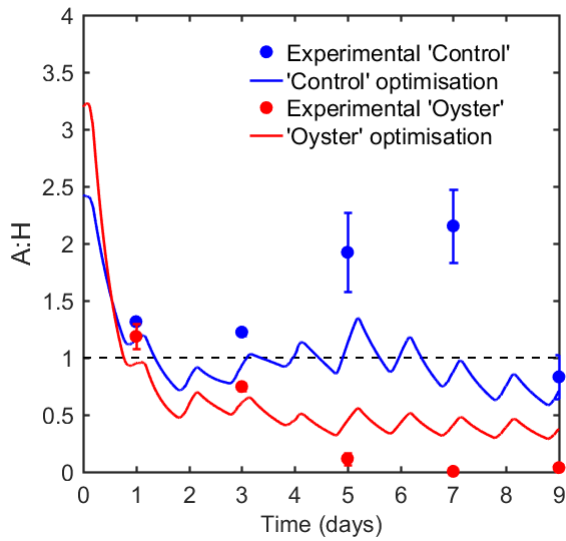


1
 2 *Figure 8: Comparison between the 'Oyster' initial simulation (dashed lines) and 'Oyster'*
 3 *optimisation (solid lines) for the (A) ammonium concentration (μM) and (B) zooplankton C*
 4 *biomass concentration (mmol C m^{-3}). The three compartments of zooplankton are represented:*
 5 *Zoo₁ (blue), Zoo₂ (red), and Zoo₃ (green).*

6

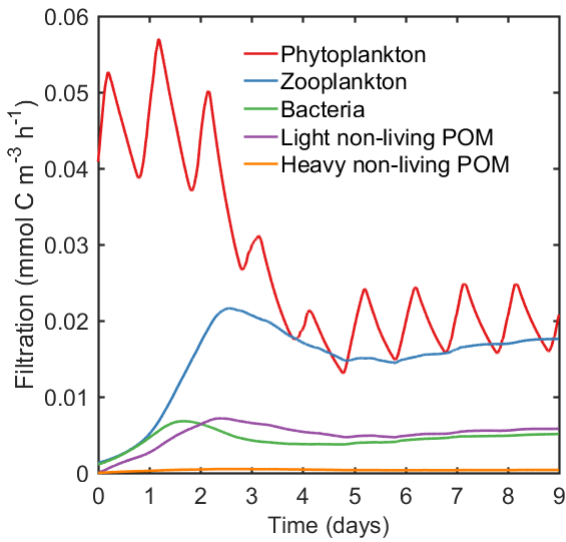


7
 8 *Figure 9: Oyster C biomass concentration (mmol C m^{-3}) for the 'Oyster' initial simulation (blue*
 9 *dashed line) and 'Oyster' optimisation (red solid line).*

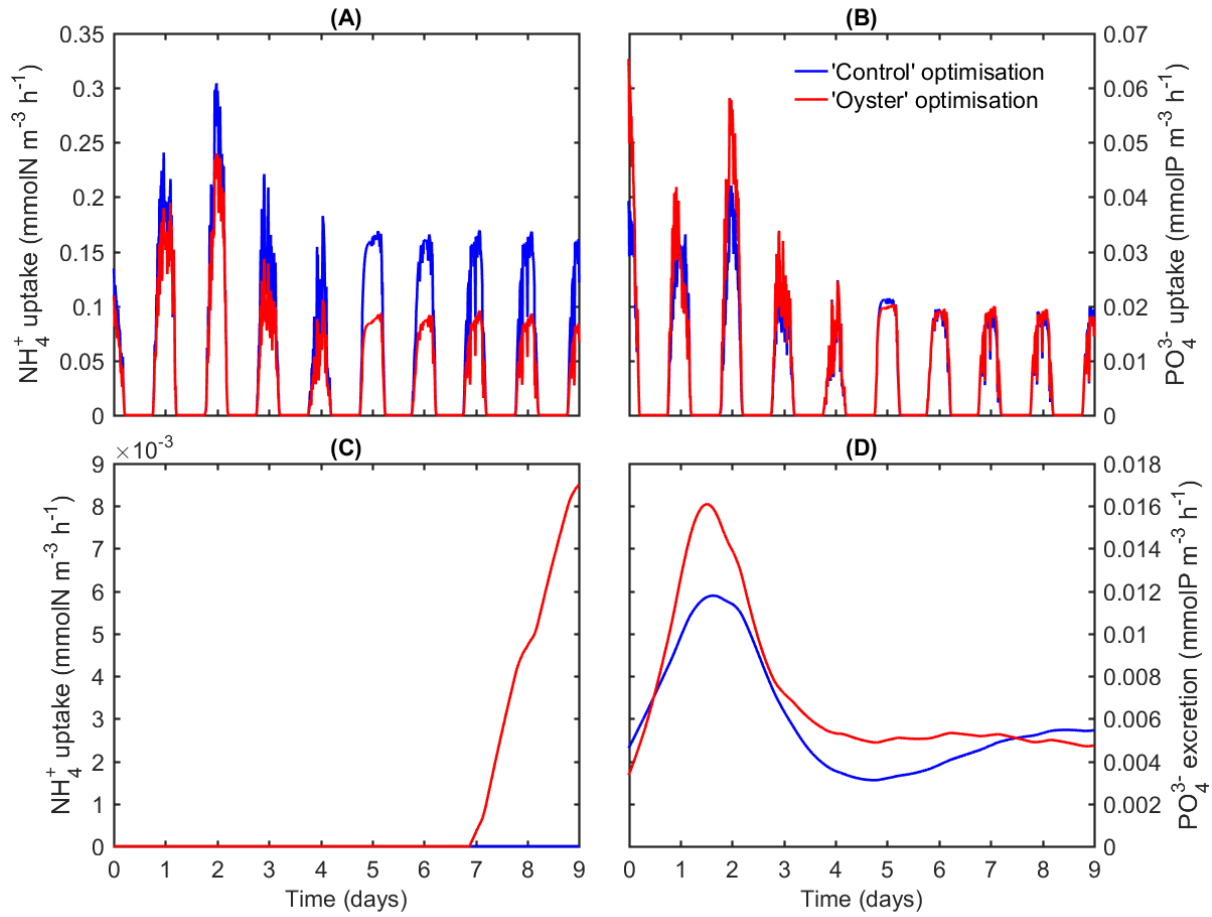


1
 2 *Figure 10: Autotroph:heterotroph (A:H) structural index comparison between the mesocosm*
 3 *experimental study (points) and biogeochemical modelling (solid lines) for the 'Control' (blue)*
 4 *and 'Oyster' (red) optimisations.*

5



6
 7 *Figure 11: Filtration by oysters of other components of the MFW: phytoplankton (red),*
 8 *zooplankton (blue), bacteria (green), light non-living POM (purple), and heavy non-living POM*
 9 *(orange).*



1
 2 *Figure 12: Comparison between the 'Control' (blue) and 'Oyster' (red) optimisations for the (A)*
 3 *uptake of ammonium by phytoplankton, (B) uptake of phosphate by phytoplankton, (C) uptake of*
 4 *ammonium by bacteria, and (D) excretion of phosphate by bacteria.*